The Smaller (SALI) and the Generalized (GALI) Alignment Index methods of chaos detection

Haris Skokos

Physics Department, Aristotle University of Thessaloniki
Thessaloniki, Greece

E-mail: hskokos@auth.gr
URL: http://users.auth.gr/hskokos/

Main contributors:
Tassos Bountis, Chris Antonopoulos, Thanos Manos, Enrico Gerlach

Outline

- **Smaller ALignment Index – SALI**
  - ✓ **Definition**
  - ✓ **Behavior for chaotic and regular motion**
  - ✓ **Applications**

- **Generalized ALignment Index – GALI**
  - ✓ **Definition - Relation to SALI**
  - ✓ **Behavior for chaotic and regular motion**
  - ✓ **Applications**
  - ✓ **Global dynamics**
  - ✓ **Motion on low-dimensional tori**

- **Summary**

Definition of Smaller Alignment Index (SALI)

Consider the 2N-dimensional phase space of a conservative dynamical system (symplectic map or Hamiltonian flow).

An orbit in that space with initial condition :

$$P(0)=(x_1(0), x_2(0),\ldots,x_{2N}(0))$$

and a deviation vector

$$v(0)=(\delta x_1(0), \delta x_2(0),\ldots, \delta x_{2N}(0))$$

The evolution in time (in maps the time is discrete and is equal to the number n of the iterations) of a deviation vector is defined by:

- **the variational equations (for Hamiltonian flows) and**
- **the equations of the tangent map (for mappings)**

Definition of SALI

We follow the evolution in time of two different initial deviation vectors ($v_1(0)$, $v_2(0)$), and define SALI (Ch.S. 2001, J. Phys. A) as:

$$SALI(t) = \min\left\{\left\|\hat{v}_1(t) + \hat{v}_2(t)\right\|, \left\|\hat{v}_1(t) - \hat{v}_2(t)\right\|\right\}$$

where

$$\hat{v}_1(t) = \frac{v_1(t)}{\left\|v_1(t)\right\|}$$

When the two vectors become collinear

$$SALI(t) \rightarrow 0$$

Behavior of SALI for chaotic motion

For chaotic orbits the two initially different deviation vectors tend to coincide with the direction defined by the maximum Lyapunov exponent.

Behavior of SALI for chaotic motion

For chaotic orbits the two initially different deviation vectors tend to coincide with the direction defined by the maximum Lyapunov exponent.

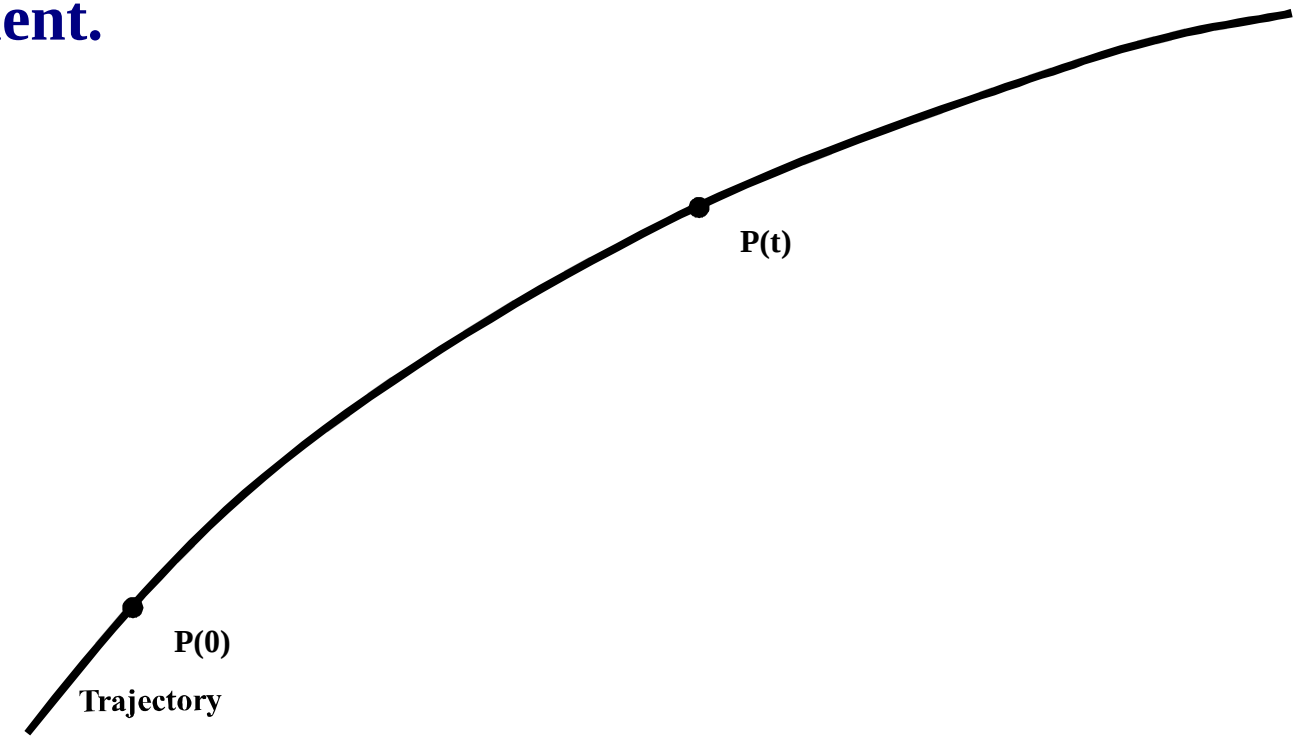

Behavior of SALI for chaotic motion

For chaotic orbits the two initially different deviation vectors tend to coincide with the direction defined by the maximum Lyapunov exponent.

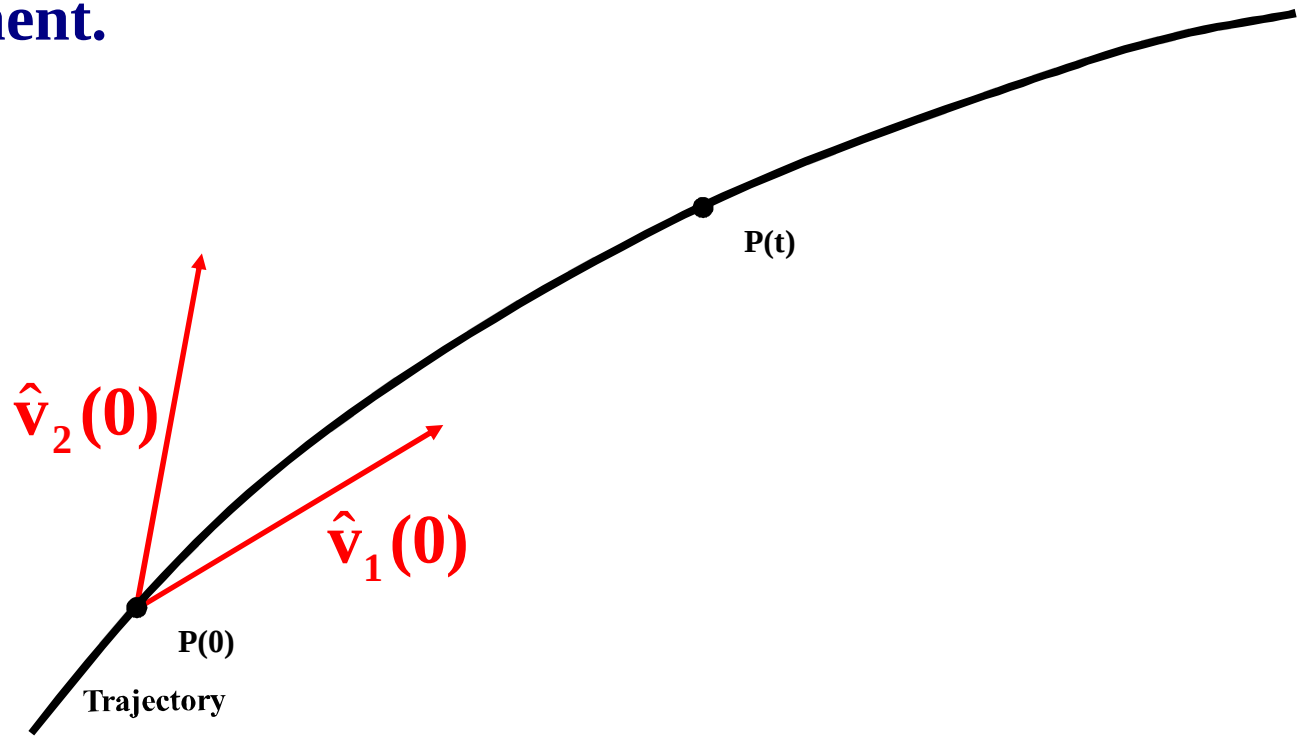

Behavior of SALI for chaotic motion

For chaotic orbits the two initially different deviation vectors tend to coincide with the direction defined by the maximum Lyapunov exponent.

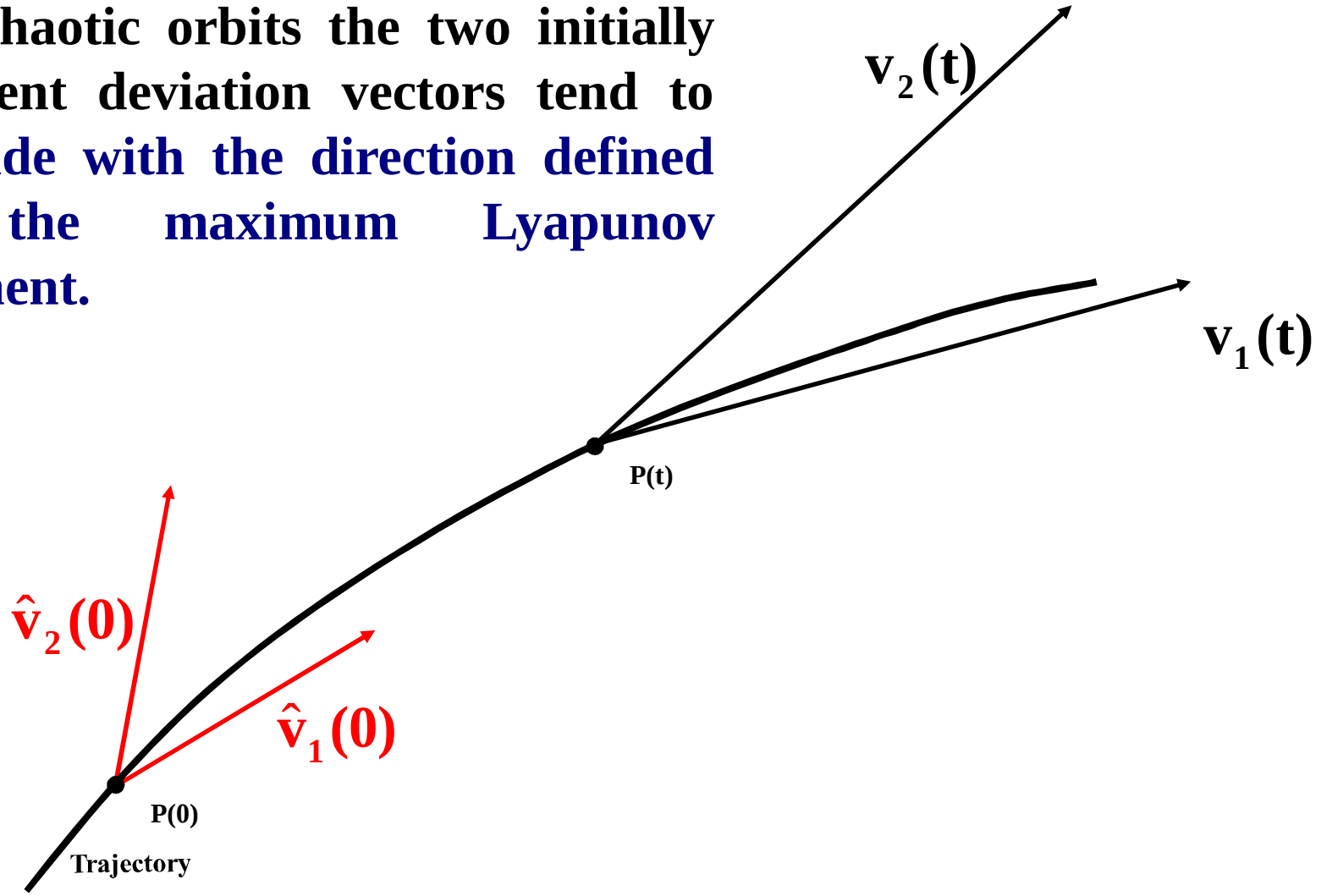

Behavior of SALI for chaotic motion

For chaotic orbits the two initially different deviation vectors tend to coincide with the direction defined by the maximum Lyapunov exponent.

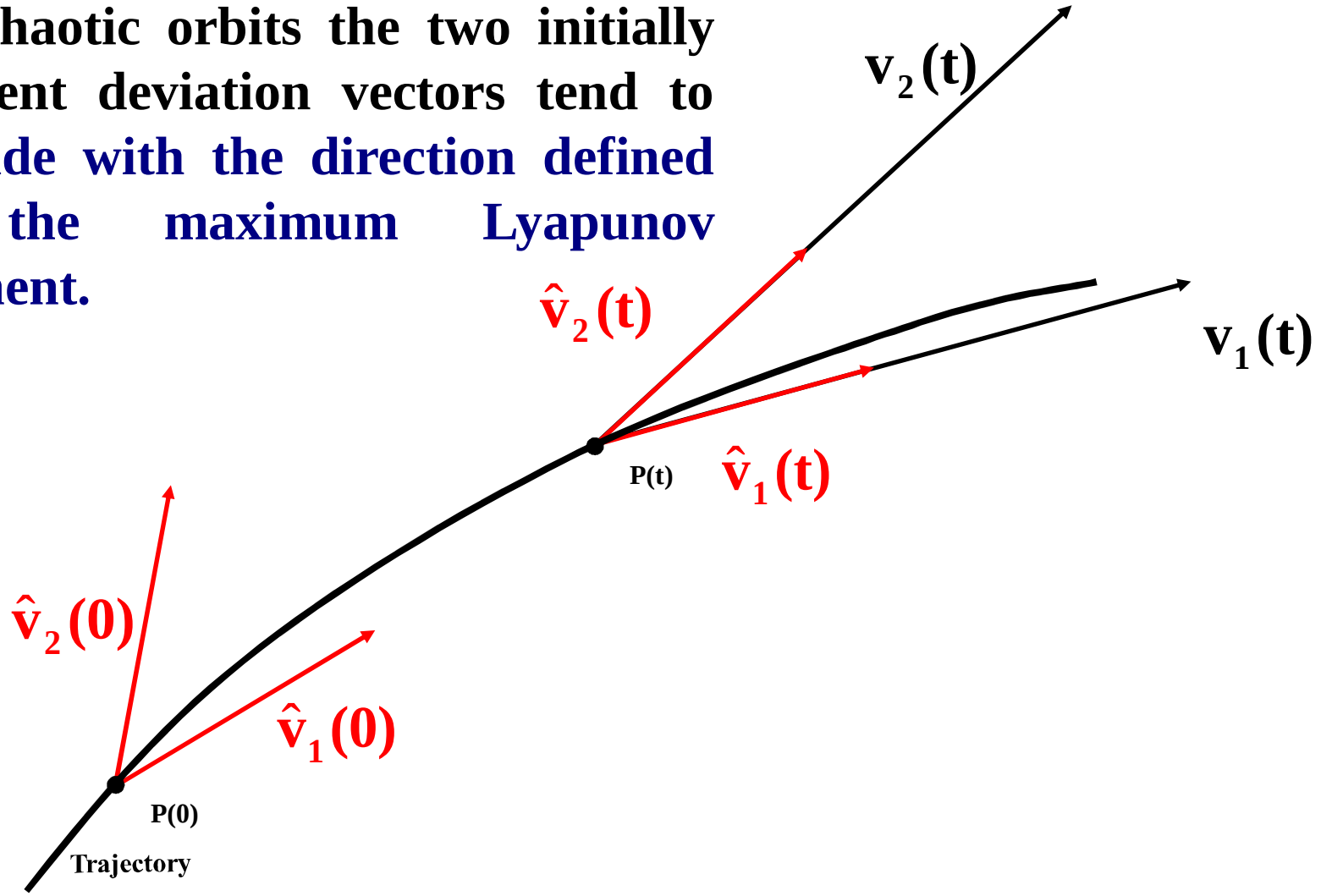

Behavior of SALI for chaotic motion

For chaotic orbits the two initially different deviation vectors tend to coincide with the direction defined by the maximum Lyapunov exponent.

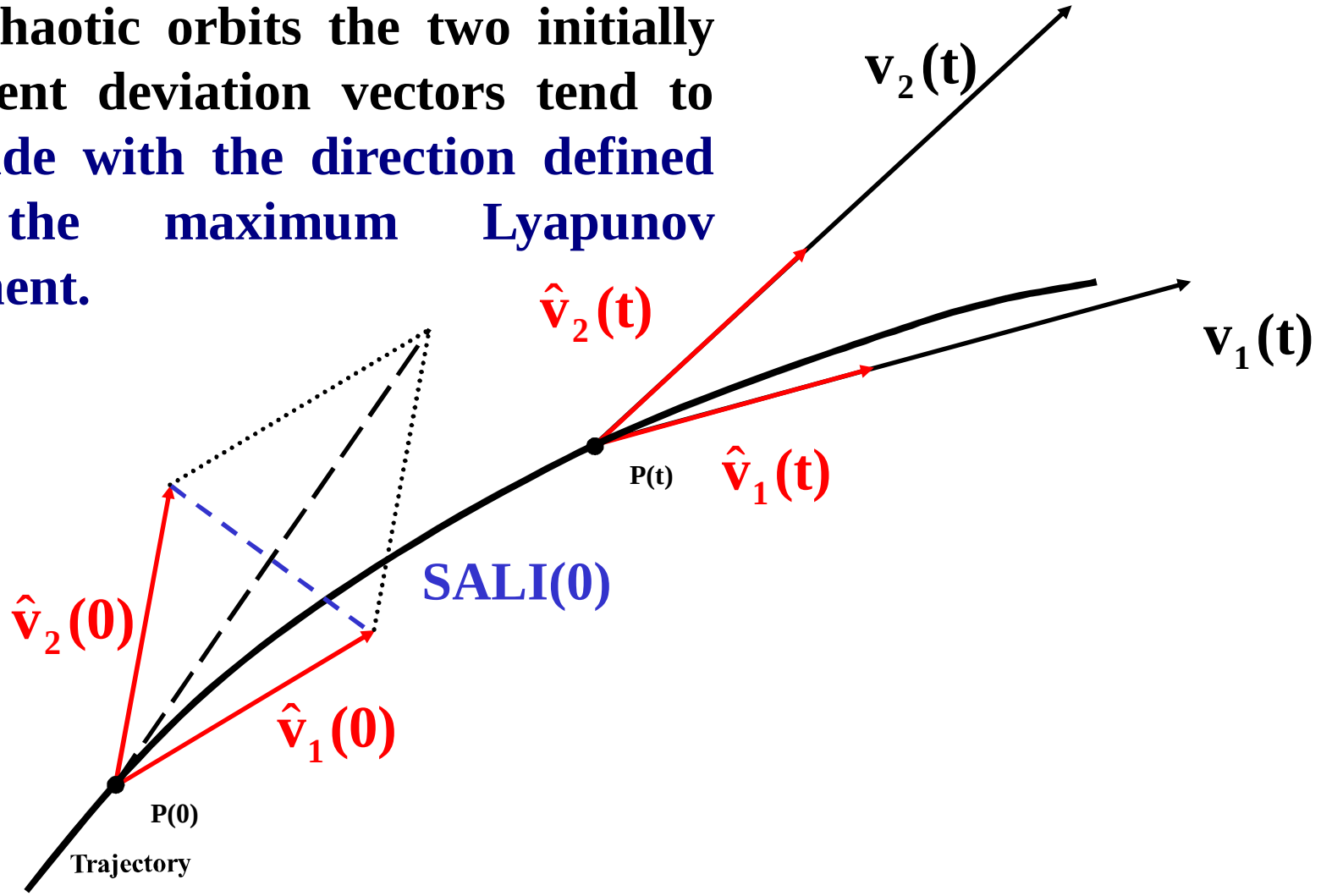

Behavior of SALI for chaotic motion

For chaotic orbits the two initially different deviation vectors tend to coincide with the direction defined by the maximum Lyapunov exponent.

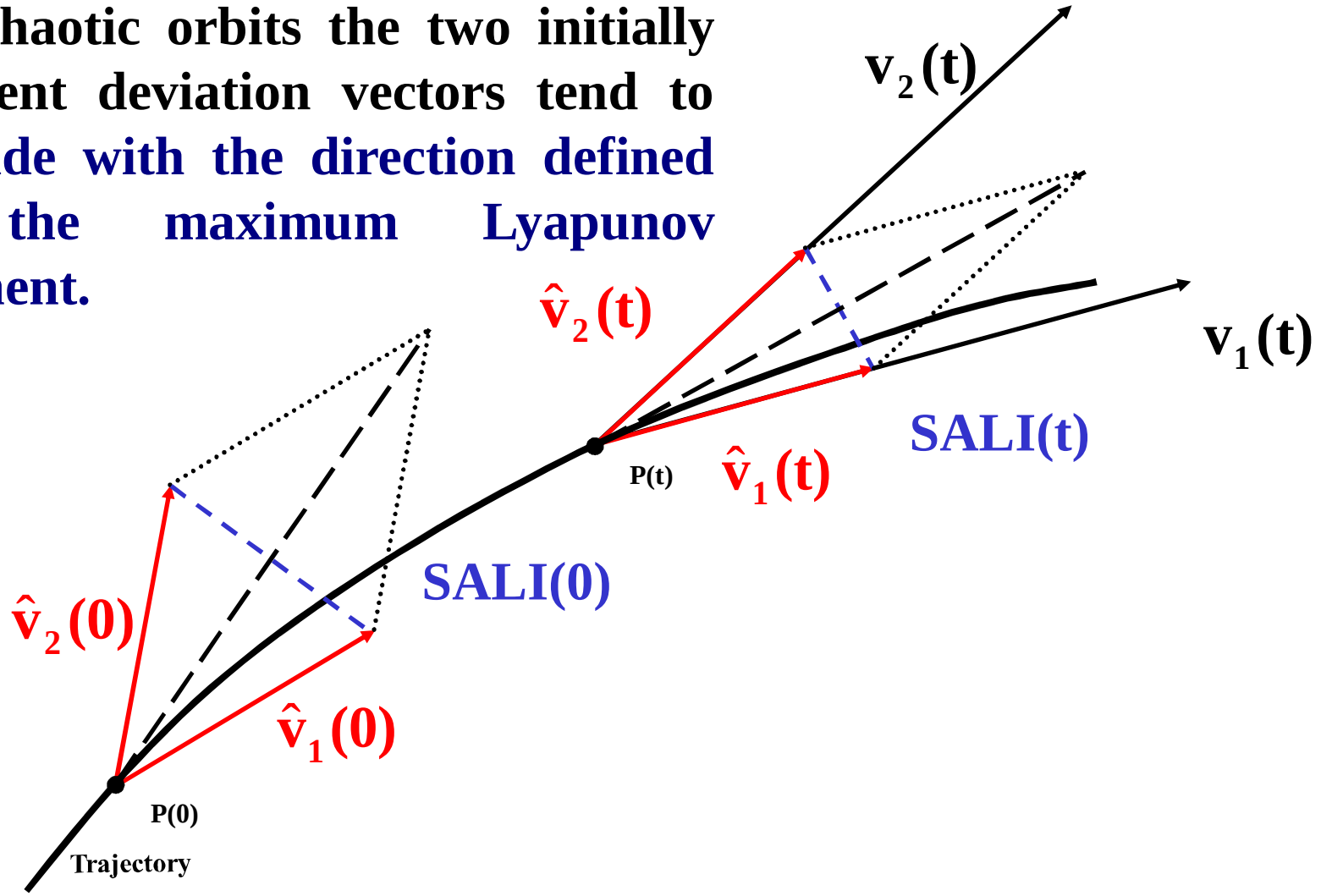

Behavior of SALI for chaotic motion

The evolution of a deviation vector can be approximated by:

$$\mathbf{v}_1(t) = \sum_{i=1}^{n} c_i^{(1)} e^{\sigma_i t} \hat{\mathbf{u}}_i \approx c_1^{(1)} e^{\sigma_1 t} \hat{\mathbf{u}}_1 + c_2^{(1)} e^{\sigma_2 t} \hat{\mathbf{u}}_2$$

where $\sigma_1 > \sigma_2 \geq \ldots \geq \sigma_n$ are the Lyapunov exponents, and $\hat{\mathbf{u}}_j$ j=1, 2, …, 2N the corresponding eigendirections.

In this approximation, we derive a leading order estimate of the ratio

$$\frac{\mathbf{v}_1(t)}{\|\mathbf{v}_1(t)\|} \approx \frac{c_1^{(1)} e^{\sigma_1 t} \hat{\mathbf{u}}_1 + c_2^{(1)} e^{\sigma_2 t} \hat{\mathbf{u}}_2}{\left|c_1^{(1)}\right| e^{\sigma_1 t}} = \pm \hat{\mathbf{u}}_1 + \frac{c_2^{(1)}}{\left|c_1^{(1)}\right|} e^{-(\sigma_1 - \sigma_2)t} \hat{\mathbf{u}}_2$$

and an analogous expression for $\mathbf{v}_2$

$$\frac{\mathbf{v}_2(t)}{\|\mathbf{v}_2(t)\|} \approx \frac{c_1^{(2)} e^{\sigma_1 t} \hat{\mathbf{u}}_1 + c_2^{(2)} e^{\sigma_2 t} \hat{\mathbf{u}}_2}{\left|c_1^{(2)}\right| e^{\sigma_1 t}} = \pm \hat{\mathbf{u}}_1 + \frac{c_2^{(2)}}{\left|c_1^{(2)}\right|} e^{-(\sigma_1 - \sigma_2)t} \hat{\mathbf{u}}_2$$

So we get:

$$\mathrm{SALI}(t) = \min\left\{ \left\| \frac{\mathbf{v}_1(t)}{\|\mathbf{v}_1(t)\|} + \frac{\mathbf{v}_2(t)}{\|\mathbf{v}_2(t)\|} \right\|, \left\| \frac{\mathbf{v}_1(t)}{\|\mathbf{v}_1(t)\|} - \frac{\mathbf{v}_2(t)}{\|\mathbf{v}_2(t)\|} \right\| \right\} \approx \left| \frac{c_2^{(1)}}{\left|c_1^{(1)}\right|} \pm \frac{c_2^{(2)}}{\left|c_1^{(2)}\right|} \right| e^{-(\sigma_1 - \sigma_2)t}$$

Behavior of SALI for chaotic motion

We test the validity of the approximation $SALI \propto e^{-(\sigma 1-\sigma 2)t}$ (Ch.S., Antonopoulos, Bountis, Vrahatis, 2004, J. Phys. A) for a chaotic orbit of the 3D Hamiltonian

$$H = \sum_{i=1}^{3} \frac{\omega_i}{2}(q_i^2 + p_i^2) + q_1^2 q_2 + q_1^2 q_3$$

with ω_1=1, ω_2=1.4142, ω_3=1.7321, H=0.09

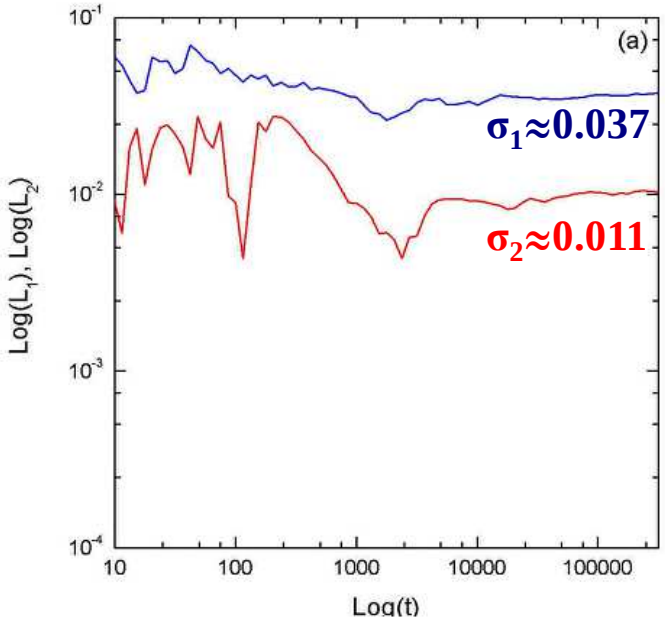

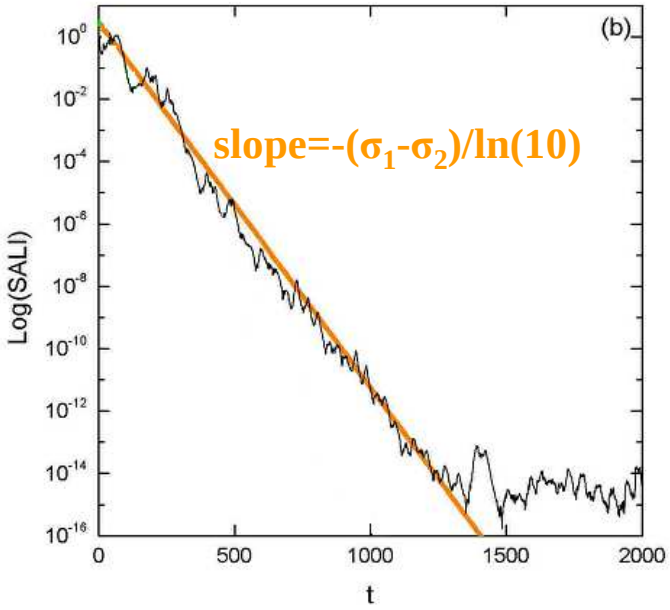

Behavior of SALI for regular motion

Regular motion occurs on a torus and two different initial deviation vectors become tangent to the torus, generally having different directions.

Behavior of SALI for regular motion

Regular motion occurs on a torus and two different initial deviation vectors become tangent to the torus, generally having different directions.

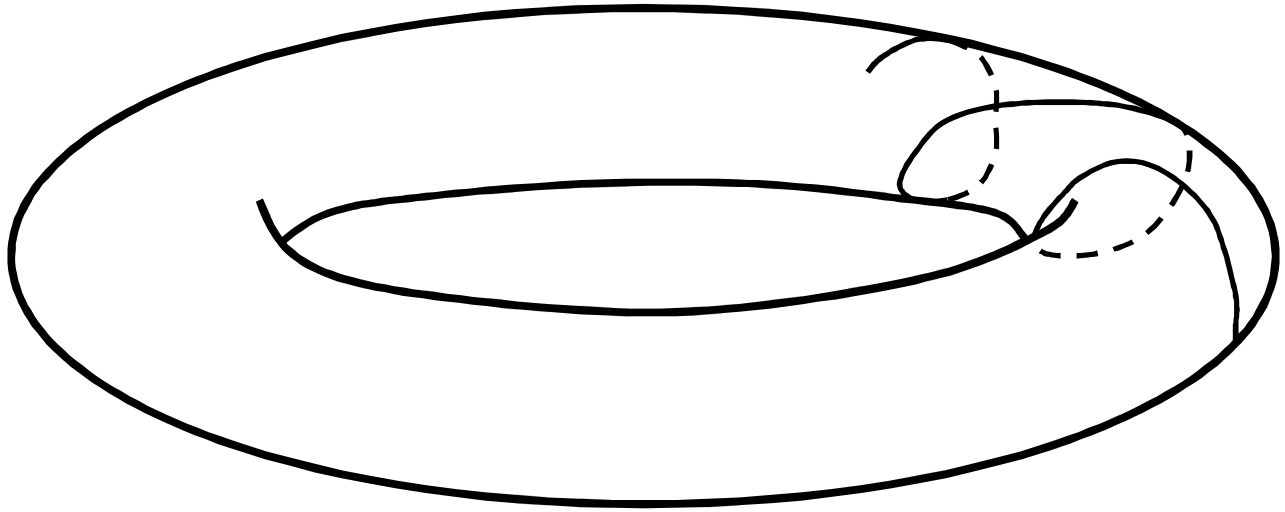

Behavior of SALI for regular motion

Regular motion occurs on a torus and two different initial deviation vectors become tangent to the torus, generally having different directions.

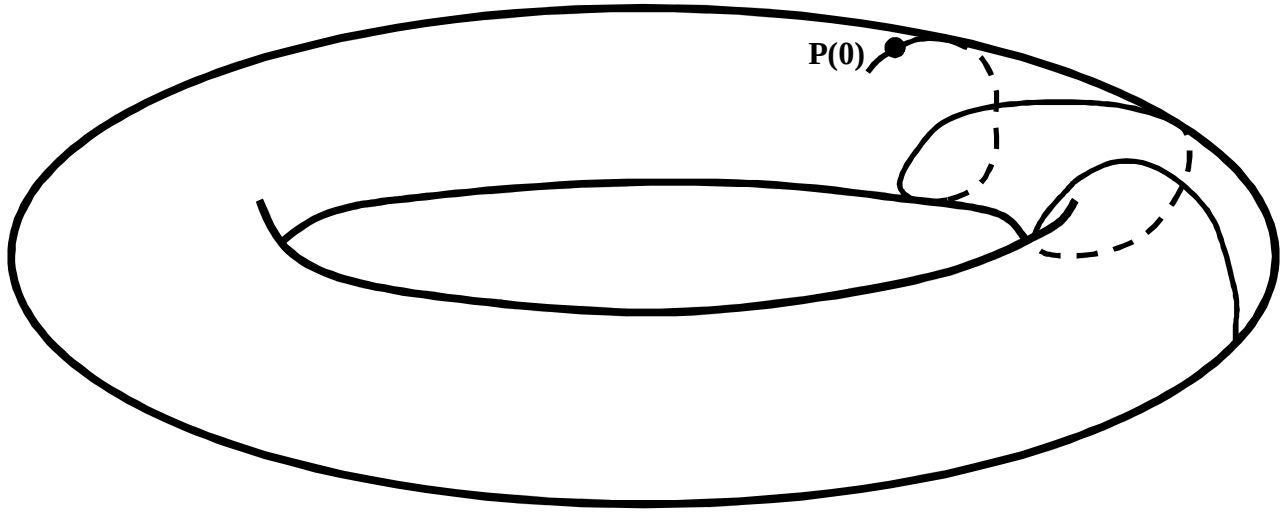

Behavior of SALI for regular motion

Regular motion occurs on a torus and two different initial deviation vectors become tangent to the torus, generally having different directions.

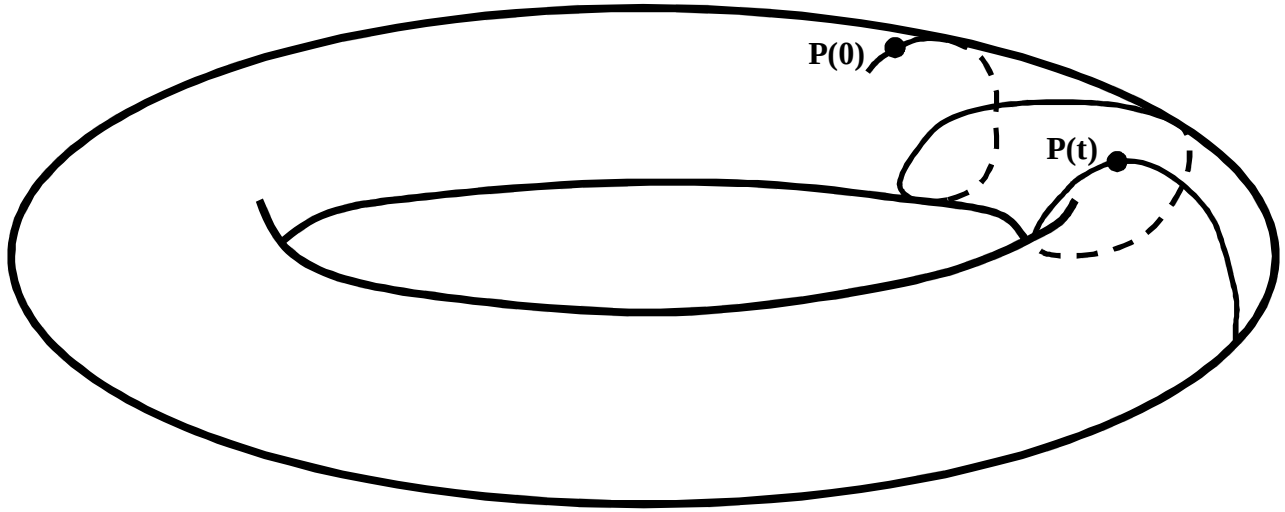

Behavior of SALI for regular motion

Regular motion occurs on a torus and two different initial deviation vectors become tangent to the torus, generally having different directions.

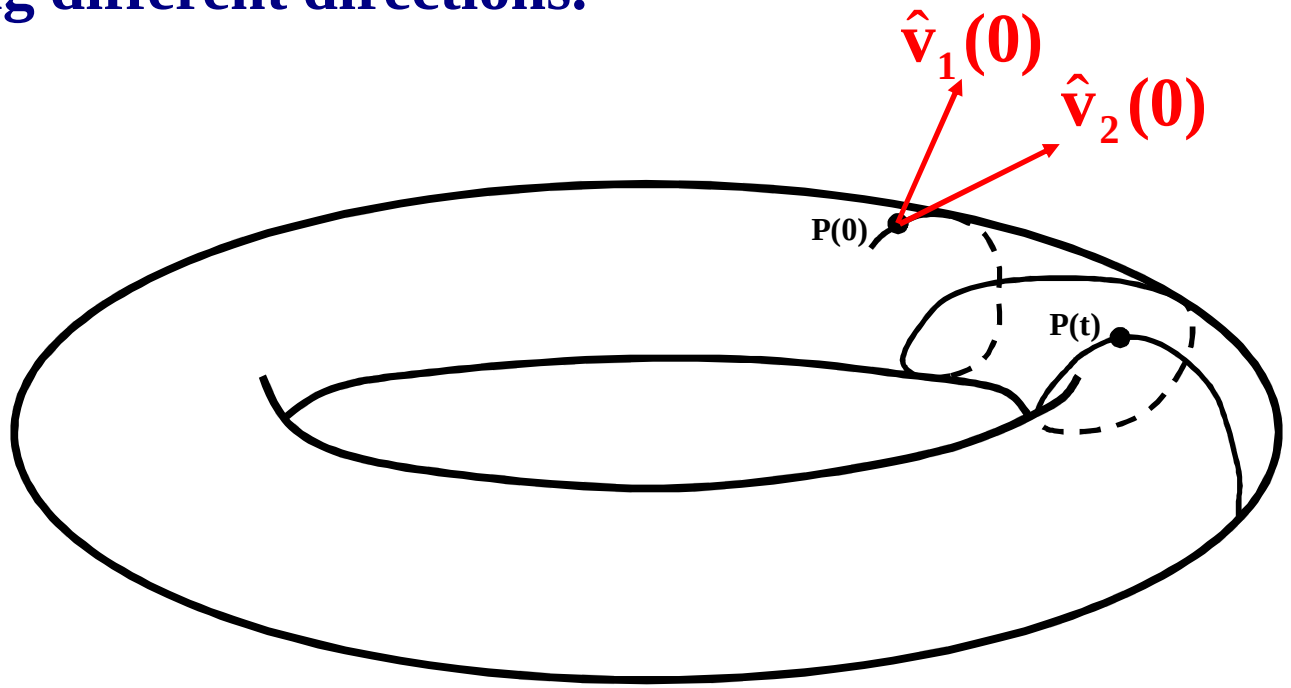

Behavior of SALI for regular motion

Regular motion occurs on a torus and two different initial deviation vectors become tangent to the torus, generally having different directions.

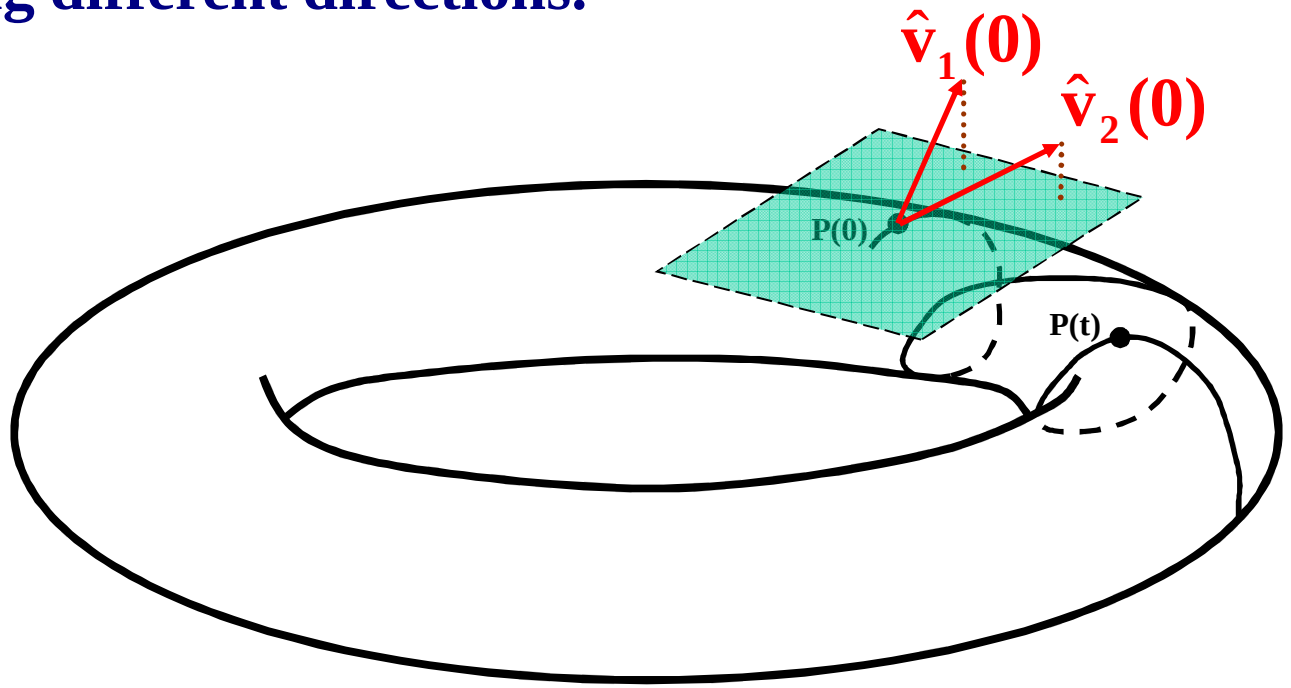

Behavior of SALI for regular motion

Regular motion occurs on a torus and two different initial deviation vectors become tangent to the torus, generally having different directions.

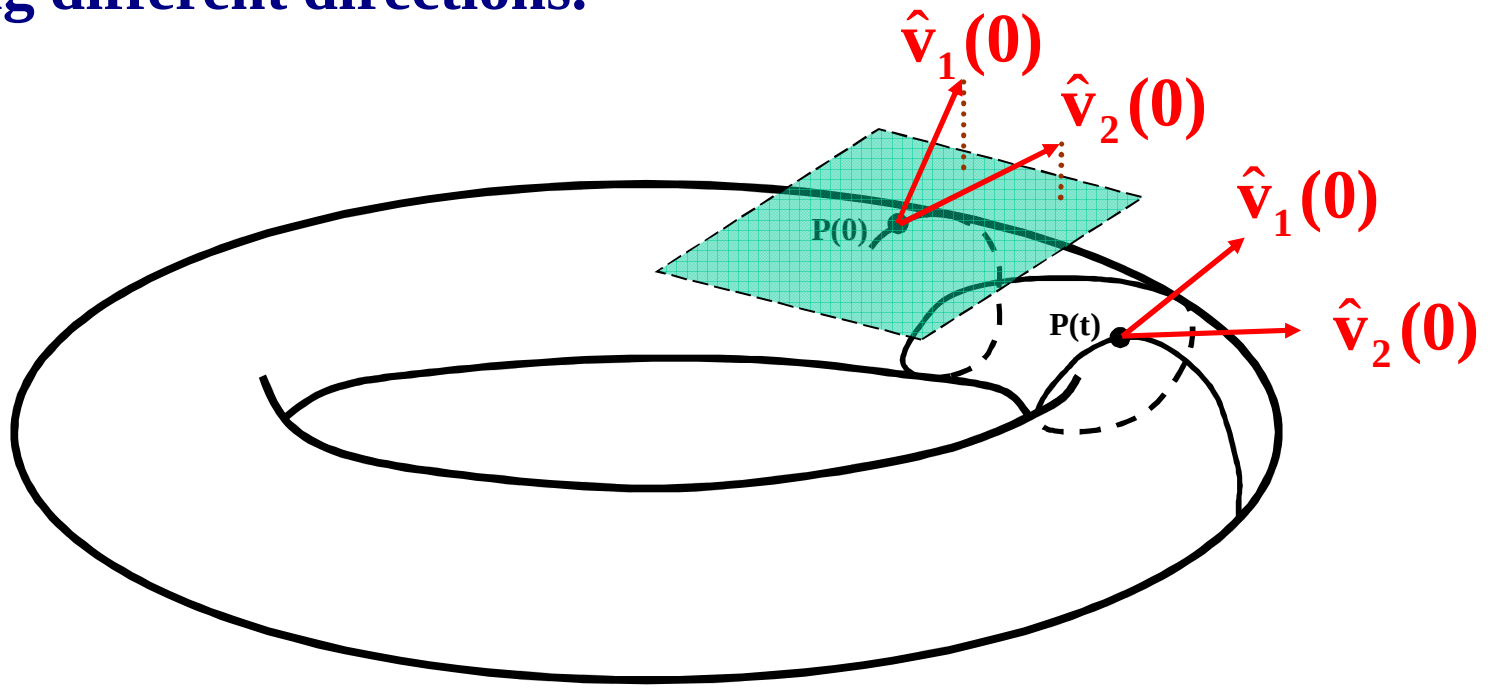

Behavior of SALI for regular motion

Regular motion occurs on a torus and two different initial deviation vectors become tangent to the torus, generally having different directions.

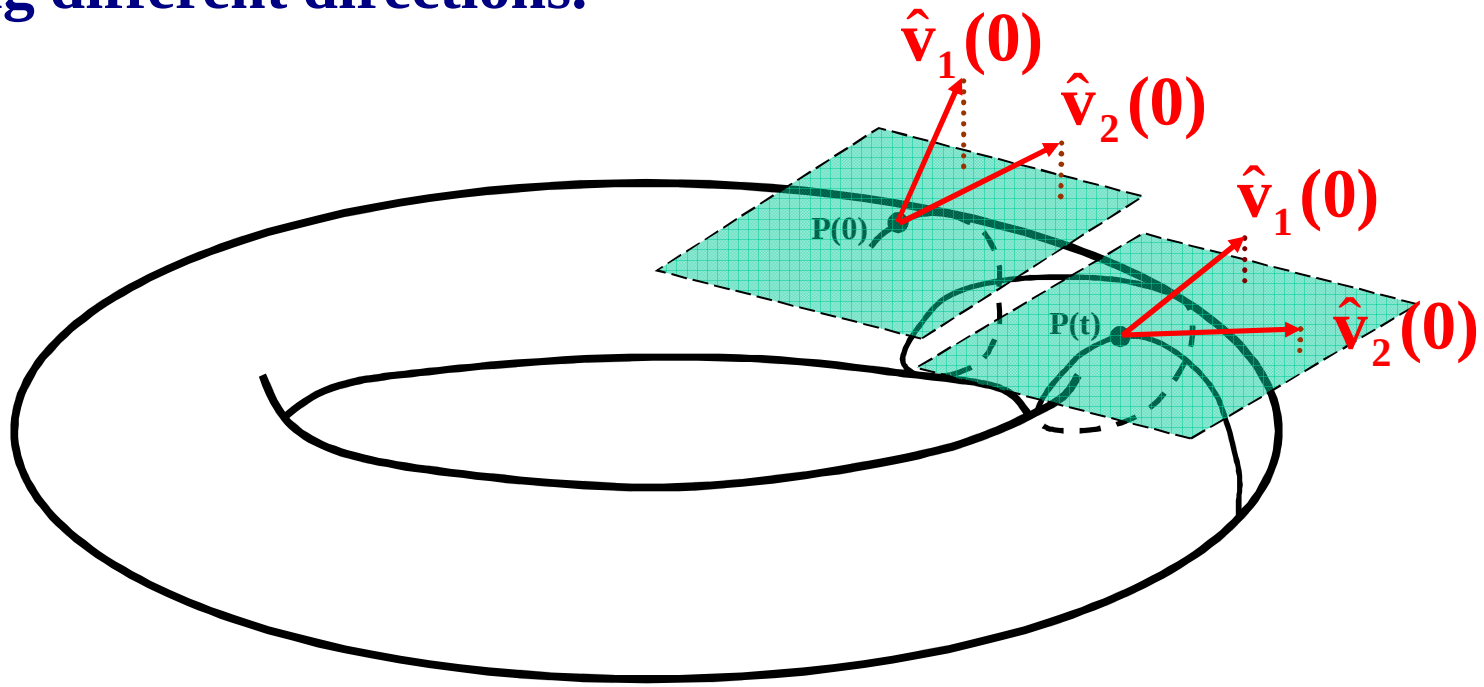

Applications – Hénon-Heiles system

As an example, we consider the 2D Hénon-Heiles system:

$$H_2 = \frac{1}{2}(p_x^2 + p_y^2) + \frac{1}{2}(x^2 + y^2) + x^2 y - \frac{1}{3}y^3$$

For E=1/8 we consider the orbits with initial conditions:
Regular orbit, x=0, y=0.55, p_x=0.2417, p_y=0
Chaotic orbit, x=0, y=-0.016, p_x=0.49974, p_y=0
Chaotic orbit, x=0, y=-0.01344, p_x=0.49982, p_y=0

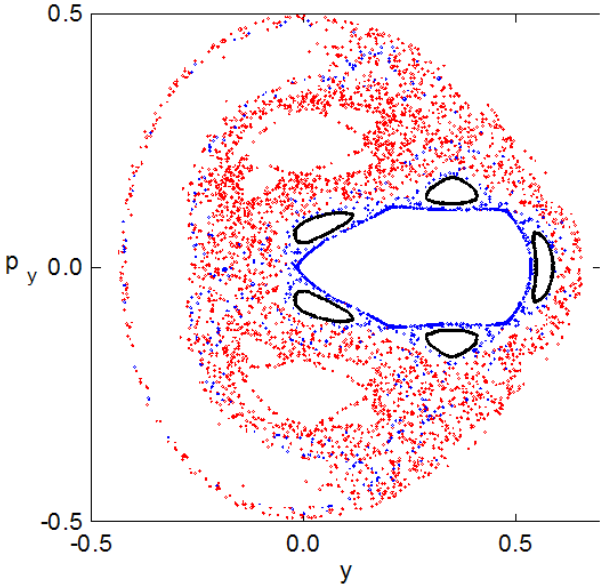

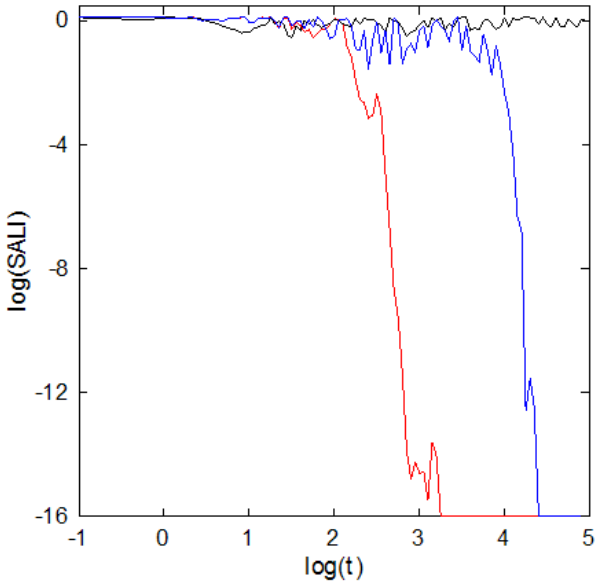

Applications – Hénon-Heiles system

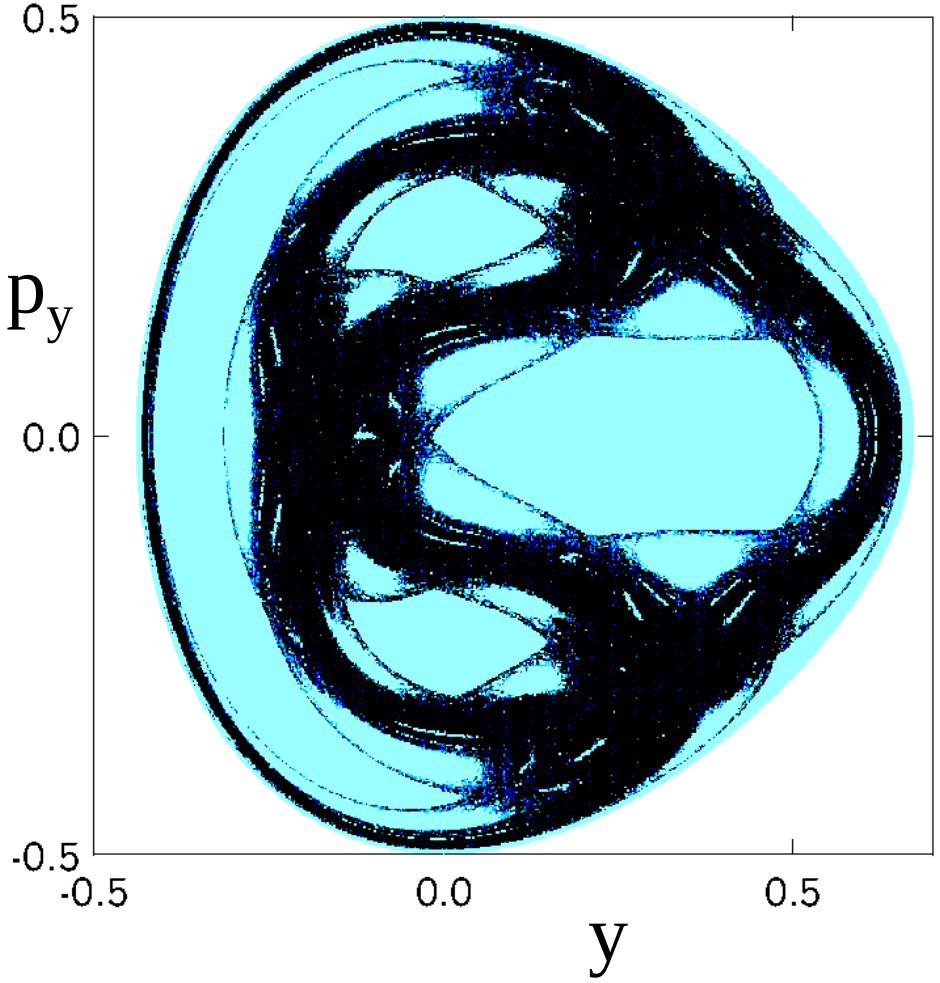

log(SALI) ≤ -12
-12 < log(SALI) ≤ -8
-8 < log(SALI) ≤ -4
-4 < log(SALI)

Applications – 4D Accelerator map

We consider the 4D symplectic map

$$\begin{pmatrix} x_1' \\ x_2' \\ x_3' \\ x_4' \end{pmatrix} = \begin{pmatrix} \cos\omega_1 & -\sin\omega_1 & 0 & 0 \\ \sin\omega_1 & \cos\omega_1 & 0 & 0 \\ 0 & 0 & \cos\omega_2 & -\sin\omega_2 \\ 0 & 0 & \sin\omega_2 & \cos\omega_2 \end{pmatrix} \times \begin{pmatrix} x_1 \\ x_2 + x_1^2 - x_3^2 \\ x_3 \\ x_4 - 2x_1x_3 \end{pmatrix}$$

describing the instantaneous sextupole 'kicks' experienced by a particle as it passes through an accelerator (Turchetti & Scandale 1991, Bountis & Tompaidis 1991, Vrahatis et al. 1996, 1997).

x_1 and x_3 are the particle's deflections from the ideal circular orbit, in the horizontal and vertical directions respectively.

x_2 and x_4 are the associated momenta

ω_1, ω_2 are related to the accelerator's tunes q_x, q_y by $\omega_1 = 2\pi q_x$, $\omega_2 = 2\pi q_y$

Our goal is to estimate the region of stability of the particle's motion, the so-called dynamic aperture of the beam (Bountis, Ch.S., 2006, Nucl. Inst Meth. Phys Res. A) and to increase its size using chaos control techniques (Boreaux, Carletti, Ch.S., Vittot, 2012, Com. Nonlin. Sci. Num. Sim. – Boreaux, Carletti, Ch.S., Papaphilippou, Vittot, 2012, Int. J. Bif. Chaos).

4D Accelerator map – "Global" study

Regions of different values of the SALI on the subspace $x_2(0)=x_4(0)=0$, after 10^5 iterations ($q_x=0.61803$ $q_y=0.4152$)

4D map

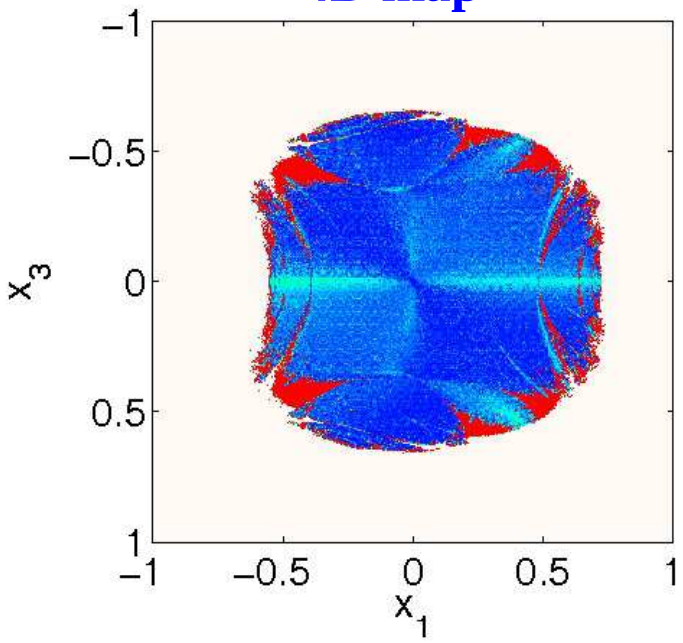

Controlled 4D map

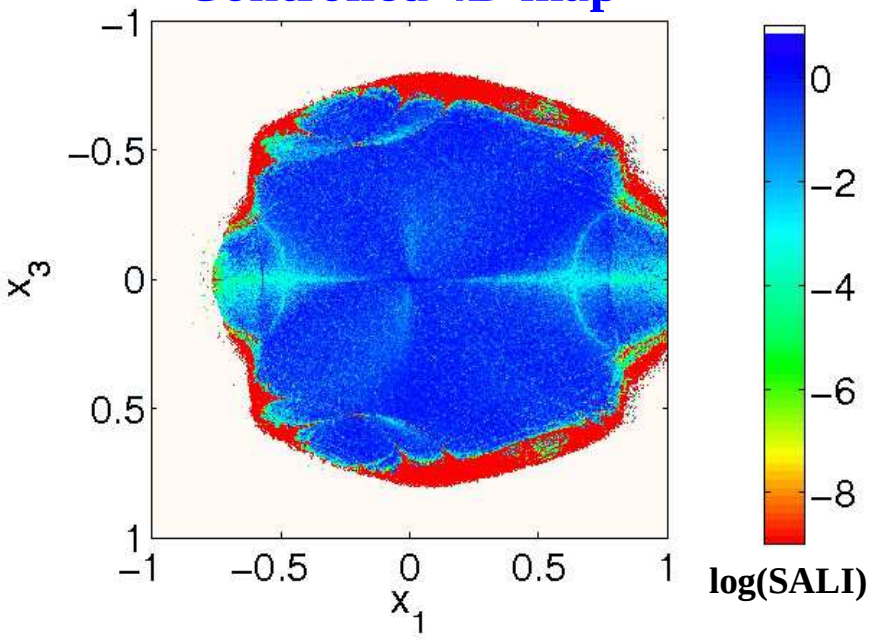

4D Accelerator map – "Global" study

Increase of the dynamic aperture

We evolve many orbits in 4D hyperspheres of radius r centered at $x_1=x_2=x_3=x_4=0$, for 10^5 iterations.

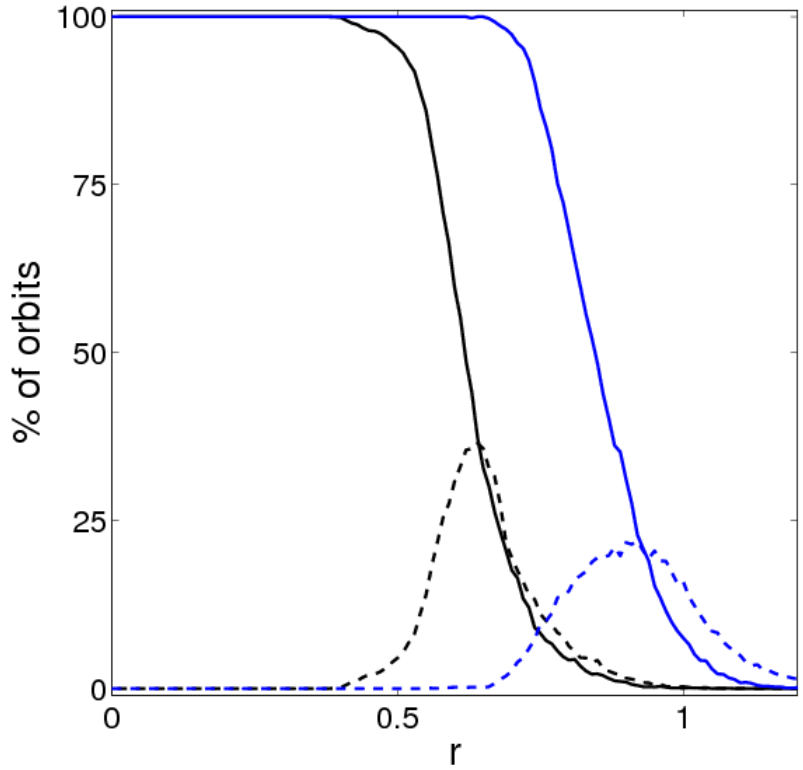

4D map

Controlled 4D map

Regular orbits

Chaotic orbits

Applications – 2D map

$$x_1' = x_1 + x_2$$
$$x_2' = x_2 - \nu \sin(x_1 + x_2) \quad \text{(mod } 2\pi\text{)}$$

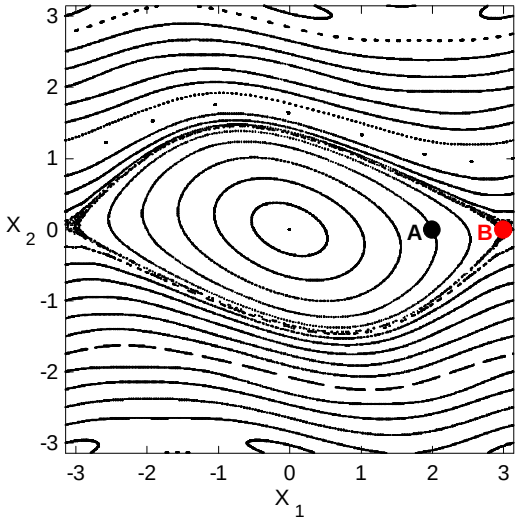

For ν=0.5 we consider the orbits:
regular orbit A *with initial conditions* $x_1=2$, $x_2=0$.
chaotic orbit B *with initial conditions* $x_1=3$, $x_2=0$.

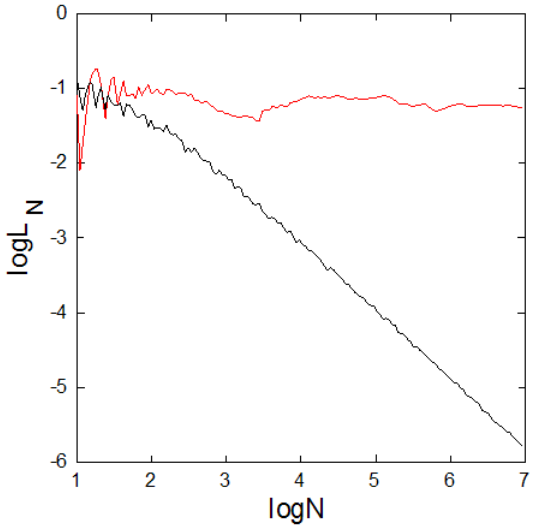

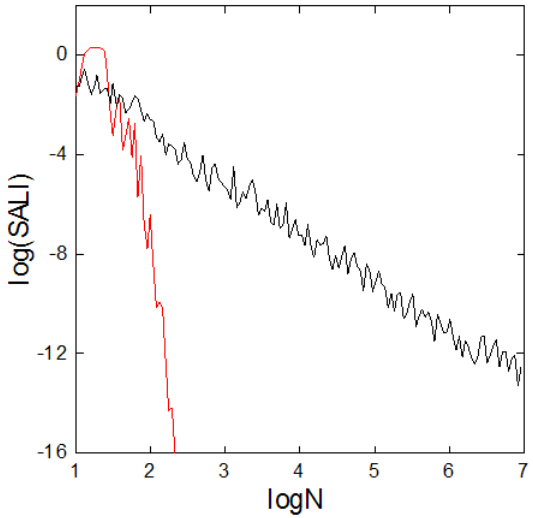

Behavior of SALI

2D maps

SALI→0 both for regular and chaotic orbits

following, however, completely different time rates which allows us to distinguish between the two cases.

Hamiltonian flows and multidimensional maps

SALI→0 for chaotic orbits

SALI→constant ≠ 0 for regular orbits

Questions

Can we generalize SALI so that the new index:

- **Can rapidly reveal the nature of chaotic orbits with $\sigma_1 \approx \sigma_2$ ($SALI \propto e^{-(\sigma 1 - \sigma 2)t}$)?**

- **Depends on several Lyapunov exponents for chaotic orbits?**

- **Exhibits power-law decay for regular orbits depending on the dimensionality of the tangent space of the reference orbit as for 2D maps?**

Definition of Generalized Alignment Index (GALI)

SALI effectively measures the ‘area’ of the parallelogram formed by the two deviation vectors.

Definition of Generalized Alignment Index (GALI)

SALI effectively measures the 'area' of the parallelogram formed by the two deviation vectors.

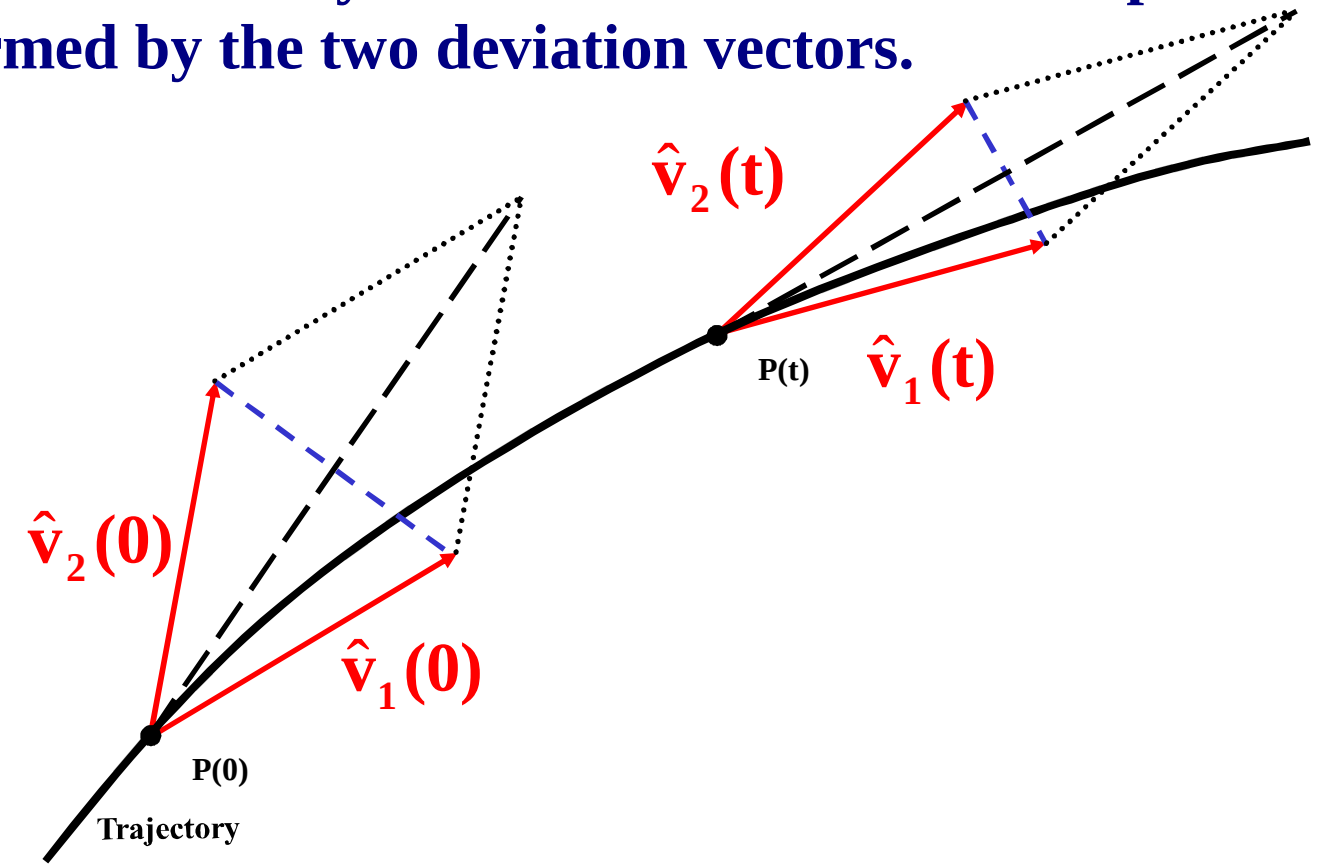

Definition of Generalized Alignment Index (GALI)

SALI effectively measures the 'area' of the parallelogram formed by the two deviation vectors.

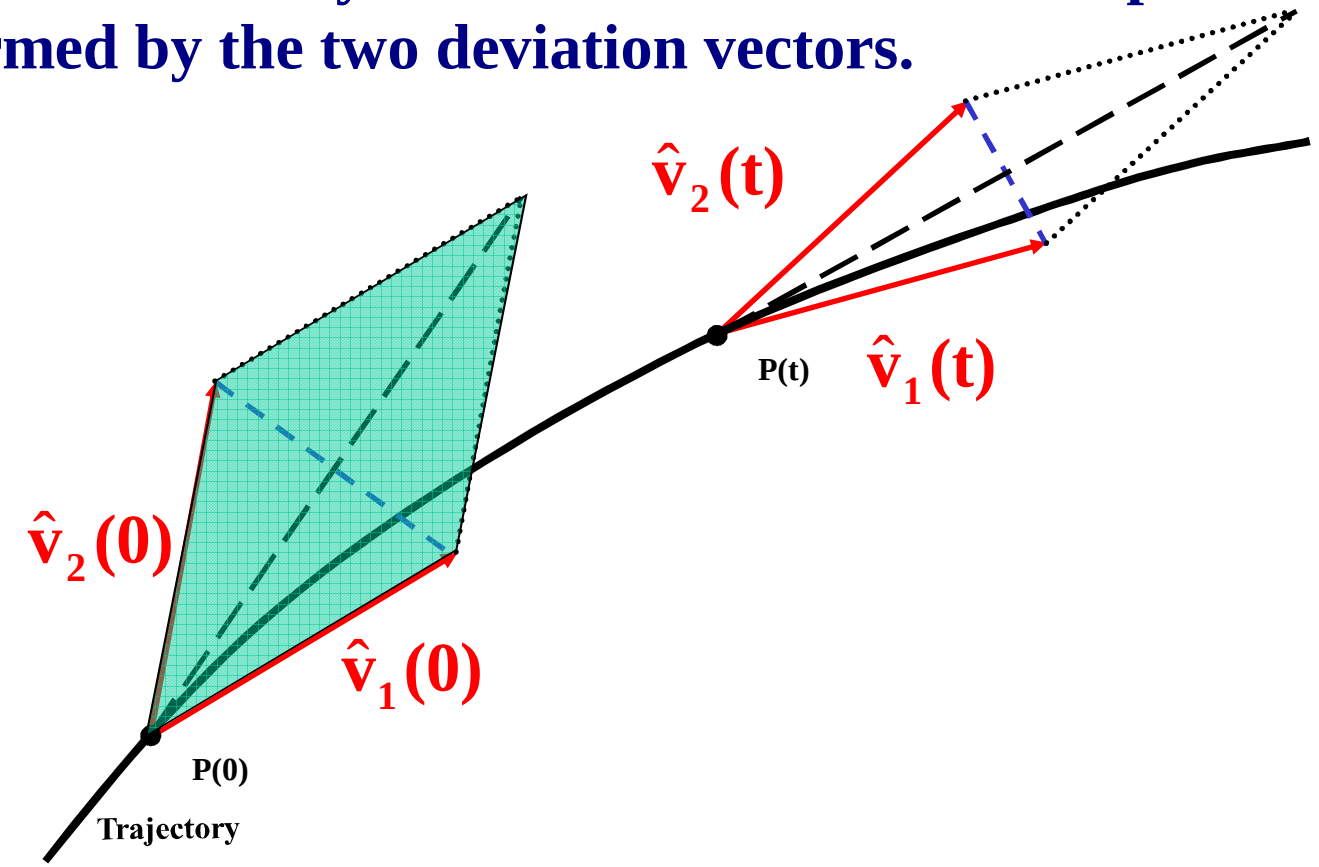

Definition of Generalized Alignment Index (GALI)

SALI effectively measures the 'area' of the parallelogram formed by the two deviation vectors.

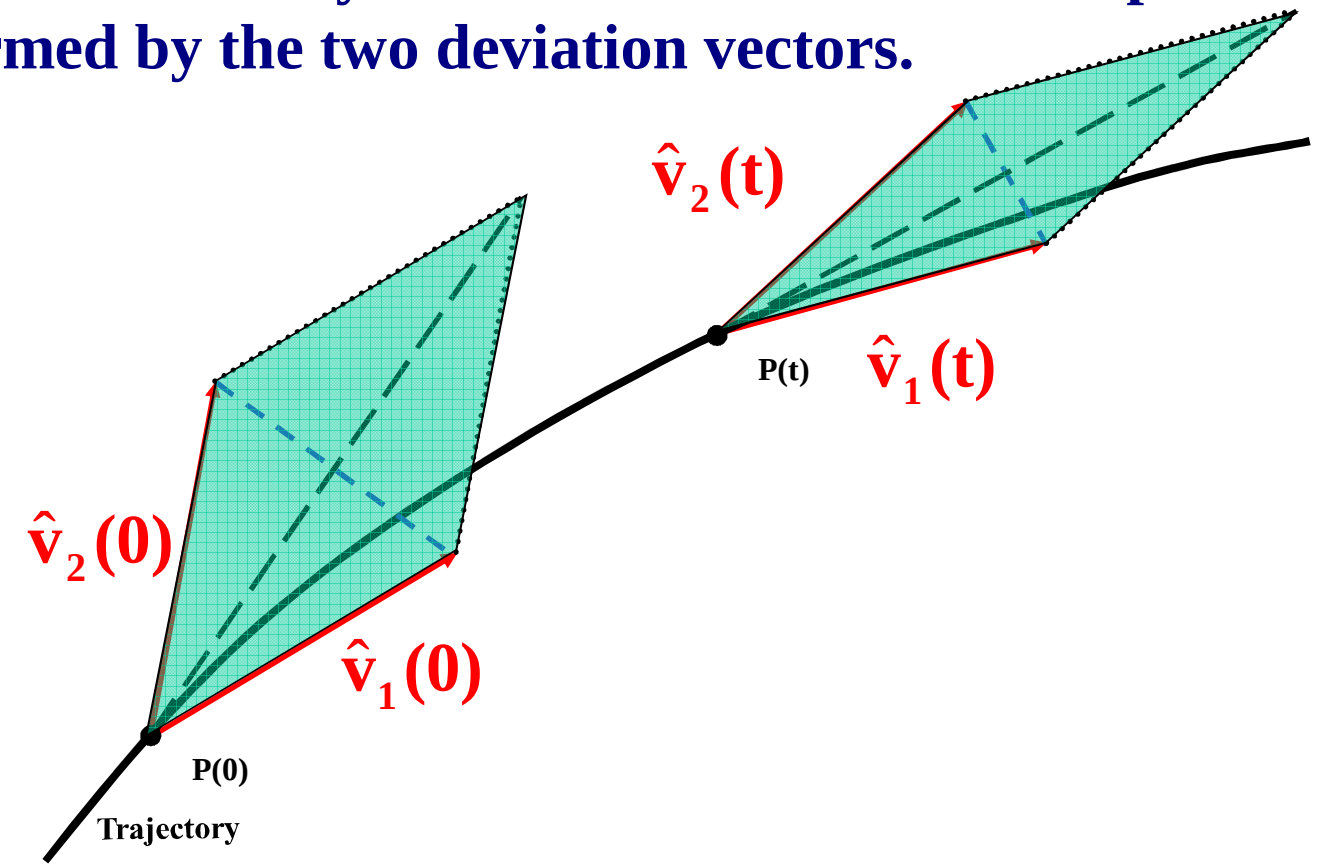

Definition of Generalized Alignment Index (GALI)

SALI effectively measures the 'area' of the parallelogram formed by the two deviation vectors.

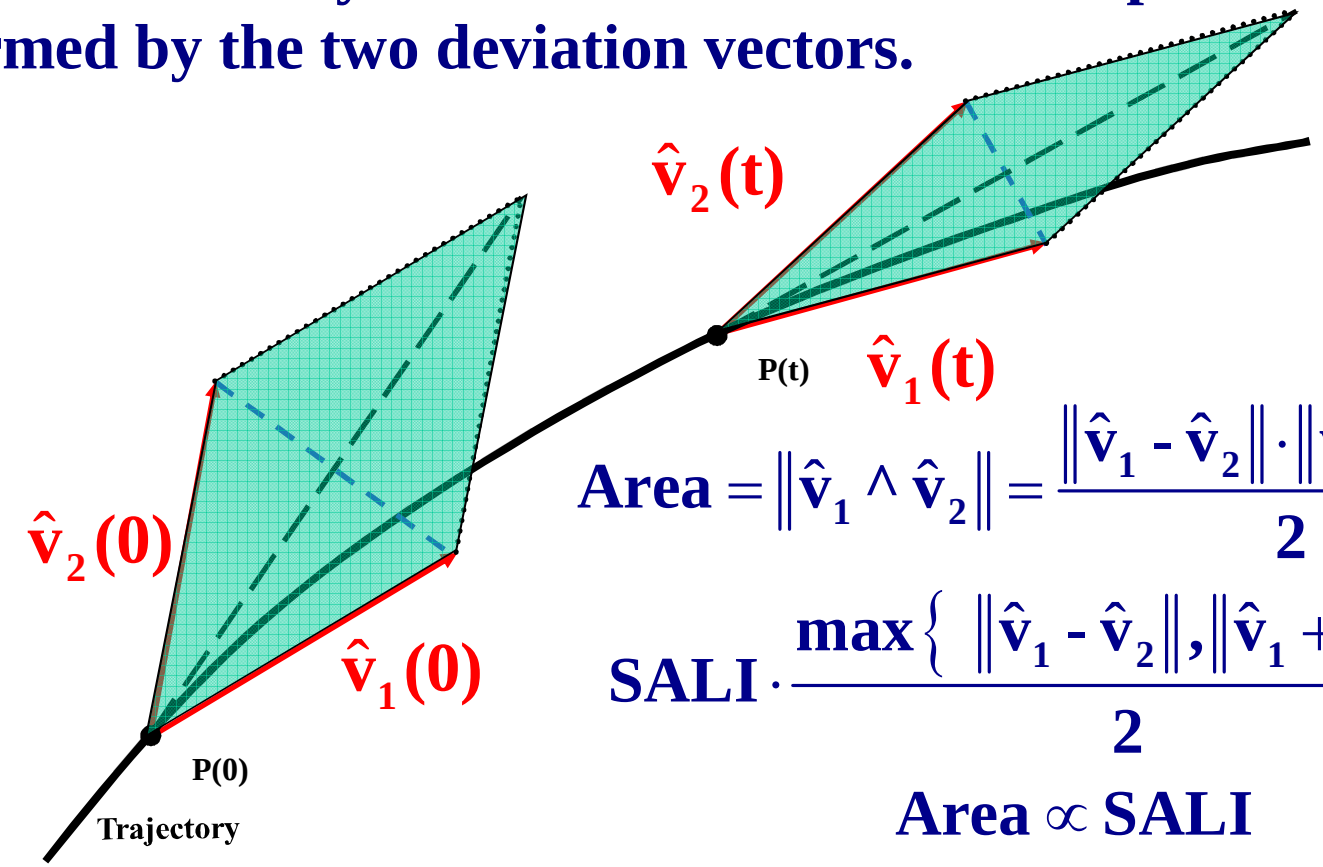

$$\text{Area} = \left\| \hat{v}_1 \wedge \hat{v}_2 \right\| = \frac{\left\| \hat{v}_1 - \hat{v}_2 \right\| \cdot \left\| \hat{v}_1 + \hat{v}_2 \right\|}{2} =$$

$$\text{SALI} \cdot \frac{\max\left\{ \left\| \hat{v}_1 - \hat{v}_2 \right\|, \left\| \hat{v}_1 + \hat{v}_2 \right\| \right\}}{2} \Rightarrow$$

$$\text{Area} \propto \text{SALI}$$

Definition of GALI

In the case of an N degree of freedom Hamiltonian system or a 2N symplectic map we follow the evolution of

k deviation vectors with $2 \leq k \leq 2N$,

and define (Ch.S., Bountis, Antonopoulos, 2007, Physica D) the Generalized Alignment Index (GALI) of order k :

$$GALI_k(t) = \left\| \hat{v}_1(t) \wedge \hat{v}_2(t) \wedge \ldots \wedge \hat{v}_k(t) \right\|$$

where

$$\hat{v}_1(t) = \frac{v_1(t)}{\left\| v_1(t) \right\|}$$

Wedge product

We consider as a basis of the 2N-dimensional tangent space of the system the usual set of orthonormal vectors:

$$\hat{e}_1 = (1,0,0,...,0),\ \hat{e}_2 = (0,1,0,...,0),\ ...,\ \hat{e}_{2N} = (0,0,0,...,1)$$

Then for k deviation vectors we have:

$$\begin{bmatrix} \hat{v}_1 \\ \hat{v}_2 \\ \vdots \\ \hat{v}_k \end{bmatrix} = \begin{bmatrix} v_{11} & v_{12} & \cdots & v_{1\,2N} \\ v_{21} & v_{22} & \cdots & v_{2\,2N} \\ \vdots & \vdots & & \vdots \\ v_{k1} & v_{k2} & \cdots & v_{k\,2N} \end{bmatrix} \cdot \begin{bmatrix} \hat{e}_1 \\ \hat{e}_2 \\ \vdots \\ \hat{e}_{2N} \end{bmatrix}$$

$$\hat{v}_1 \wedge \hat{v}_2 \wedge \cdots \wedge \hat{v}_k = \sum_{1 \le i_1 < i_2 < \cdots < i_k \le 2N} \begin{vmatrix} v_{1\,i_1} & v_{1\,i_2} & \cdots & v_{1\,i_k} \\ v_{2\,i_1} & v_{2\,i_2} & \cdots & v_{2\,i_k} \\ \vdots & \vdots & & \vdots \\ v_{k\,i_1} & v_{k\,i_2} & \cdots & v_{k\,i_k} \end{vmatrix} \hat{e}_{i_1} \wedge \hat{e}_{i_2} \wedge \cdots \wedge \hat{e}_{i_k}$$

Norm of wedge product

We define as ‘norm’ of the wedge product the quantity :

$$\left\|\hat{\mathbf{v}}_1 \wedge \hat{\mathbf{v}}_2 \wedge \cdots \wedge \hat{\mathbf{v}}_k\right\| = \left\{ \sum_{1 \le i_1 < i_2 < \cdots < i_k \le 2N} \begin{vmatrix} v_{1\,i_1} & v_{1\,i_2} & \cdots & v_{1\,i_k} \\ v_{2\,i_1} & v_{2\,i_2} & \cdots & v_{2\,i_k} \\ \vdots & \vdots & & \vdots \\ v_{k\,i_1} & v_{k\,i_2} & \cdots & v_{k\,i_k} \end{vmatrix}^2 \right\}^{1/2}$$

Computation of GALI - Example

Let us compute $GALI_3$ in the case of 2D Hamiltonian system (4-dimensional phase space).

$$\begin{bmatrix} \hat{v}_1 \\ \hat{v}_2 \\ \hat{v}_3 \end{bmatrix} = \begin{bmatrix} v_{11} & v_{12} & v_{13} & v_{14} \\ v_{21} & v_{22} & v_{23} & v_{24} \\ v_{31} & v_{32} & v_{33} & v_{34} \end{bmatrix} \cdot \begin{bmatrix} \hat{e}_1 \\ \hat{e}_2 \\ \hat{e}_3 \\ \hat{e}_4 \end{bmatrix}$$

Computation of GALI - Example

Let us compute $GALI_3$ in the case of 2D Hamiltonian system (4-dimensional phase space).

$$\begin{bmatrix} \hat{v}_1 \\ \hat{v}_2 \\ \hat{v}_3 \end{bmatrix} = \begin{bmatrix} v_{11} & v_{12} & v_{13} & v_{14} \\ v_{21} & v_{22} & v_{23} & v_{24} \\ v_{31} & v_{32} & v_{33} & v_{34} \end{bmatrix} \cdot \begin{bmatrix} \hat{e}_1 \\ \hat{e}_2 \\ \hat{e}_3 \\ \hat{e}_4 \end{bmatrix}$$

Columns 1 2 3

$$GALI_3 = \left\| \hat{v}_1 \wedge \hat{v}_2 \wedge \hat{v}_3 \right\| = \left\{ \begin{vmatrix} v_{11} & v_{12} & v_{13} \\ v_{21} & v_{22} & v_{23} \\ v_{31} & v_{32} & v_{33} \end{vmatrix}^2 + \right.$$

Computation of GALI - Example

Let us compute $GALI_3$ in the case of 2D Hamiltonian system (4-dimensional phase space).

$$\begin{bmatrix} \hat{v}_1 \\ \hat{v}_2 \\ \hat{v}_3 \end{bmatrix} = \begin{bmatrix} v_{11} & v_{12} & v_{13} & v_{14} \\ v_{21} & v_{22} & v_{23} & v_{24} \\ v_{31} & v_{32} & v_{33} & v_{34} \end{bmatrix} \cdot \begin{bmatrix} \hat{e}_1 \\ \hat{e}_2 \\ \hat{e}_3 \\ \hat{e}_4 \end{bmatrix}$$

$$GALI_3 = \left\| \hat{v}_1 \wedge \hat{v}_2 \wedge \hat{v}_3 \right\| = \left\{ \begin{vmatrix} v_{11} & v_{12} & v_{13} \\ v_{21} & v_{22} & v_{23} \\ v_{31} & v_{32} & v_{33} \end{vmatrix}^2 + \begin{vmatrix} v_{11} & v_{12} & v_{14} \\ v_{21} & v_{22} & v_{24} \\ v_{31} & v_{32} & v_{34} \end{vmatrix}^2 + \right.$$

Columns: 1 2 3 and 1 2 4

Computation of GALI - Example

Let us compute $GALI_3$ in the case of 2D Hamiltonian system (4-dimensional phase space).

$$\begin{bmatrix} \hat{v}_1 \\ \hat{v}_2 \\ \hat{v}_3 \end{bmatrix} = \begin{bmatrix} v_{11} & v_{12} & v_{13} & v_{14} \\ v_{21} & v_{22} & v_{23} & v_{24} \\ v_{31} & v_{32} & v_{33} & v_{34} \end{bmatrix} \cdot \begin{bmatrix} \hat{e}_1 \\ \hat{e}_2 \\ \hat{e}_3 \\ \hat{e}_4 \end{bmatrix}$$

$$GALI_3 = \left\| \hat{v}_1 \wedge \hat{v}_2 \wedge \hat{v}_3 \right\| = \left\{ \begin{vmatrix} v_{11} & v_{12} & v_{13} \\ v_{21} & v_{22} & v_{23} \\ v_{31} & v_{32} & v_{33} \end{vmatrix}^2 + \begin{vmatrix} v_{11} & v_{12} & v_{14} \\ v_{21} & v_{22} & v_{24} \\ v_{31} & v_{32} & v_{34} \end{vmatrix}^2 + \right.$$

$$\left. \begin{vmatrix} v_{11} & v_{13} & v_{14} \\ v_{21} & v_{23} & v_{24} \\ v_{31} & v_{33} & v_{34} \end{vmatrix}^2 + \right.$$

Columns: 1 2 3 | 1 2 4 | 1 3 4

Computation of GALI - Example

Let us compute $GALI_3$ in the case of 2D Hamiltonian system (4-dimensional phase space).

$$\begin{bmatrix} \hat{v}_1 \\ \hat{v}_2 \\ \hat{v}_3 \end{bmatrix} = \begin{bmatrix} v_{11} & v_{12} & v_{13} & v_{14} \\ v_{21} & v_{22} & v_{23} & v_{24} \\ v_{31} & v_{32} & v_{33} & v_{34} \end{bmatrix} \cdot \begin{bmatrix} \hat{e}_1 \\ \hat{e}_2 \\ \hat{e}_3 \\ \hat{e}_4 \end{bmatrix}$$

$$GALI_3 = \left\| \hat{v}_1 \wedge \hat{v}_2 \wedge \hat{v}_3 \right\| = \left\{ \begin{vmatrix} v_{11} & v_{12} & v_{13} \\ v_{21} & v_{22} & v_{23} \\ v_{31} & v_{32} & v_{33} \end{vmatrix}^2 + \begin{vmatrix} v_{11} & v_{12} & v_{14} \\ v_{21} & v_{22} & v_{24} \\ v_{31} & v_{32} & v_{34} \end{vmatrix}^2 + \right.$$

$$\left. \begin{vmatrix} v_{11} & v_{13} & v_{14} \\ v_{21} & v_{23} & v_{24} \\ v_{31} & v_{33} & v_{34} \end{vmatrix}^2 + \begin{vmatrix} v_{12} & v_{13} & v_{14} \\ v_{22} & v_{23} & v_{24} \\ v_{32} & v_{33} & v_{34} \end{vmatrix}^2 \right\}^{1/2}$$

Columns: 1 2 3 | 1 2 4 | 1 3 4 | 2 3 4

Efficient computation of GALI

For k deviation vectors:

$$\begin{bmatrix} \hat{\mathbf{v}}_1 \\ \hat{\mathbf{v}}_2 \\ \vdots \\ \hat{\mathbf{v}}_k \end{bmatrix} = \begin{bmatrix} \mathbf{v}_{11} & \mathbf{v}_{12} & \cdots & \mathbf{v}_{1\,2N} \\ \mathbf{v}_{21} & \mathbf{v}_{22} & \cdots & \mathbf{v}_{2\,2N} \\ \vdots & \vdots & & \vdots \\ \mathbf{v}_{k1} & \mathbf{v}_{k2} & \cdots & \mathbf{v}_{k\,2N} \end{bmatrix} \cdot \begin{bmatrix} \hat{\mathbf{e}}_1 \\ \hat{\mathbf{e}}_2 \\ \vdots \\ \hat{\mathbf{e}}_{2N} \end{bmatrix} = \mathbf{A} \cdot \begin{bmatrix} \hat{\mathbf{e}}_1 \\ \hat{\mathbf{e}}_2 \\ \vdots \\ \hat{\mathbf{e}}_{2N} \end{bmatrix}$$

the ‘norm’ of the wedge product is given by:

$$\left\| \hat{\mathbf{v}}_1 \wedge \hat{\mathbf{v}}_2 \wedge \cdots \wedge \hat{\mathbf{v}}_k \right\| = \left\{ \sum_{1 \le i_1 < i_2 < \cdots < i_k \le 2N} \begin{vmatrix} \mathbf{v}_{1\,i_1} & \mathbf{v}_{1\,i_2} & \cdots & \mathbf{v}_{1\,i_k} \\ \mathbf{v}_{2\,i_1} & \mathbf{v}_{2\,i_2} & \cdots & \mathbf{v}_{2\,i_k} \\ \vdots & \vdots & & \vdots \\ \mathbf{v}_{k\,i_1} & \mathbf{v}_{k\,i_2} & \cdots & \mathbf{v}_{k\,i_k} \end{vmatrix}^2 \right\}^{1/2} = \sqrt{\det(\mathbf{A} \cdot \mathbf{A}^{\mathrm{T}})}$$

Efficient computation of GALI

From Singular Value Decomposition (SVD) of A^T we get:

$$A^T = U \cdot W \cdot V^T$$

where U is a column-orthogonal 2N×k matrix ($U^T \cdot U = I$), V^T is a k×k orthogonal matrix ($V \cdot V^T = I$), and W is a diagonal k×k matrix with positive or zero elements, the so-called singular values. So, we get:

$$\det(A \cdot A^T) = \det(V \cdot W^T \cdot U^T \cdot U \cdot W \cdot V^T) = \det(V \cdot W \cdot I \cdot W \cdot V^T) =$$

$$\det(V \cdot W^2 \cdot V^T) = \det(V \cdot \mathrm{diag}(w_1^2, w_2^2, \ldots w_k^2) \cdot V^T) = \prod_{i=1}^{k} w_i^2$$

Thus, $GALI_k$ is computed by (Ch.S., Bountis, Antonopoulos, 2008, Eur. Phys. J. Sp. Top):

$$GALI_k = \sqrt{\det(A \cdot A^T)} = \prod_{i=1}^{k} w_i \Rightarrow \log\left(GALI_k\right) = \sum_{i=1}^{k} \log\left(w_i\right)$$

Behavior of $GALI_k$ for chaotic motion

$GALI_k$ $(2 \leq k \leq 2N)$ tends exponentially to zero with exponents that involve the values of the first k largest Lyapunov exponents $\sigma_1, \sigma_2, \ldots, \sigma_k$:

$$GALI_k(t) \propto e^{-\left[(\sigma_1-\sigma_2)+(\sigma_1-\sigma_3)+\ldots+(\sigma_1-\sigma_k)\right]t}$$

The above relation is valid even if some Lyapunov exponents are equal, or very close to each other.

Behavior of $GALI_k$ for chaotic motion

N particles Fermi-Pasta-Ulam (FPU) system:

$$H = \frac{1}{2}\sum_{i=1}^{N} p_i^2 + \sum_{i=0}^{N}\left[\frac{1}{2}(q_{i+1} - q_i)^2 + \frac{\beta}{4}(q_{i+1} - q_i)^4\right]$$

with fixed boundary conditions, N=8 and β=1.5.

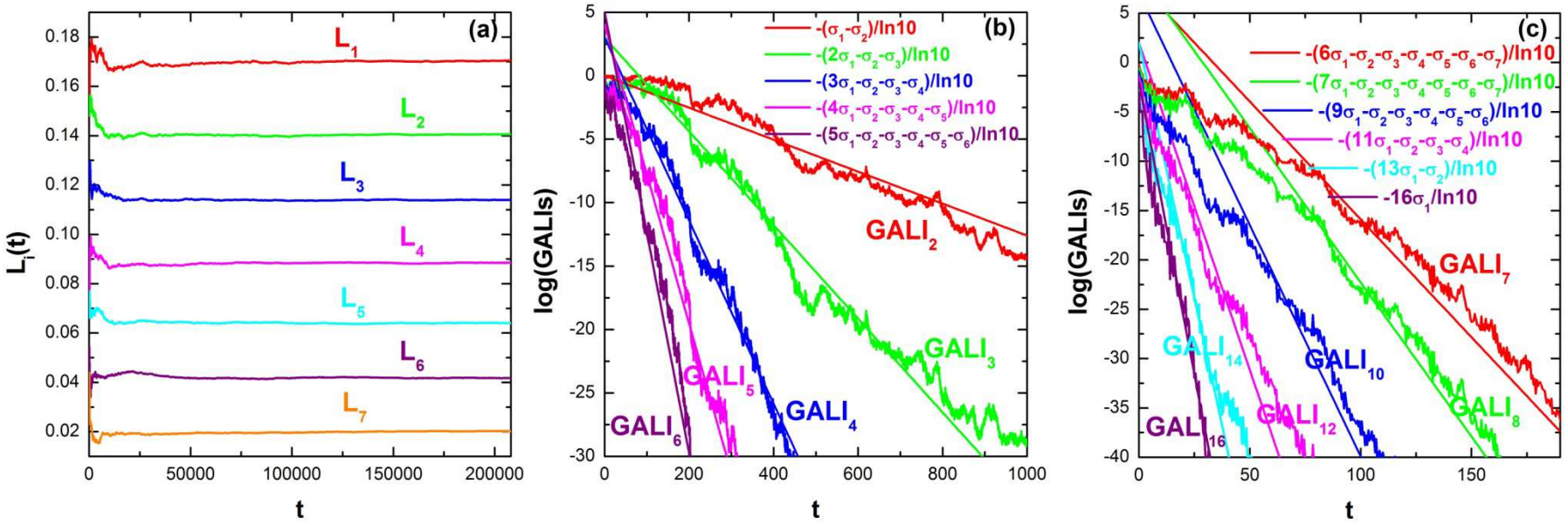

Behavior of $GALI_k$ for regular motion

If the motion occurs on an s-dimensional torus with s≤N then the behavior of $GALI_k$ is given by (Ch.S., Bountis, Antonopoulos, 2008, Eur. Phys. J. Sp. Top.):

$$GALI_k(t) \propto \begin{cases} \text{constant} & \text{if} \quad 2 \le k \le s \\ \dfrac{1}{t^{k-s}} & \text{if} \quad s < k \le 2N - s \\ \dfrac{1}{t^{2(k-N)}} & \text{if} \quad 2N - s < k \le 2N \end{cases}$$

while in the common case with s=N we have :

$$GALI_k(t) \propto \begin{cases} \text{constant} & \text{if} \quad 2 \le k \le N \\ \dfrac{1}{t^{2(k-N)}} & \text{if} \quad N < k \le 2N \end{cases}$$

Behavior of $GALI_k$ for regular motion

N=8 FPU system: The unperturbed Hamiltonian (β=0) is written as a sum of the so-called **harmonic energies E_i:**

$$E_i = \frac{1}{2}\left(P_i^2 + \omega_i^2 Q_i^2\right),\ i = 1,...,N$$

with:

$$Q_i = \sqrt{\frac{2}{N+1}}\sum_{k=1}^{N} q_k \sin\left(\frac{ki\pi}{N+1}\right),\ P_i = \sqrt{\frac{2}{N+1}}\sum_{k=1}^{N} p_k \sin\left(\frac{ki\pi}{N+1}\right),\ \omega_i = 2\sin\left(\frac{i\pi}{2(N+1)}\right)$$

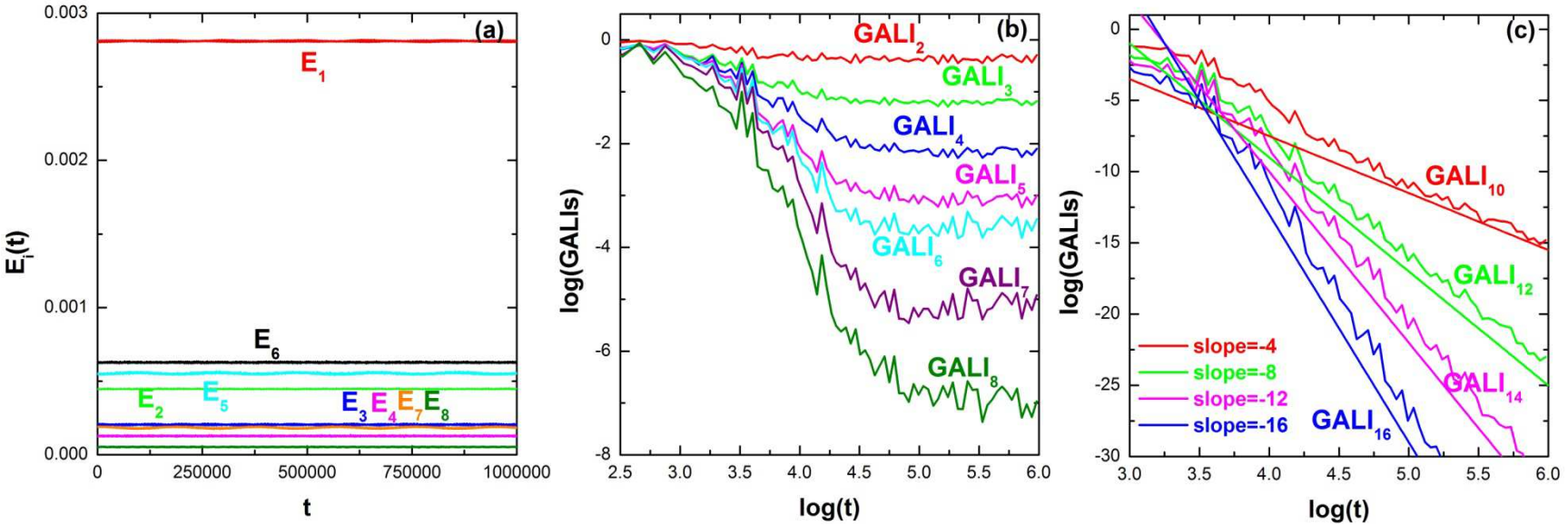

Global dynamics

- **$GALI_2$ (practically equivalent to the use of SALI)**

- **$GALI_N$**

Chaotic motion: $GALI_N \to 0$ (exponential decay)

Regular motion: $GALI_N \to$ constant$\neq 0$

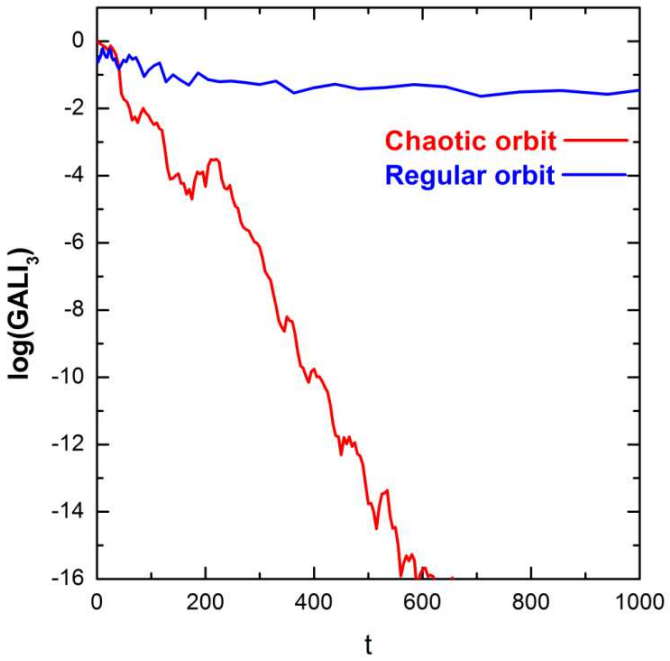

3D Hamiltonian

Subspace $q_3=p_3=0$, $p_2 \geq 0$ for t=1000.

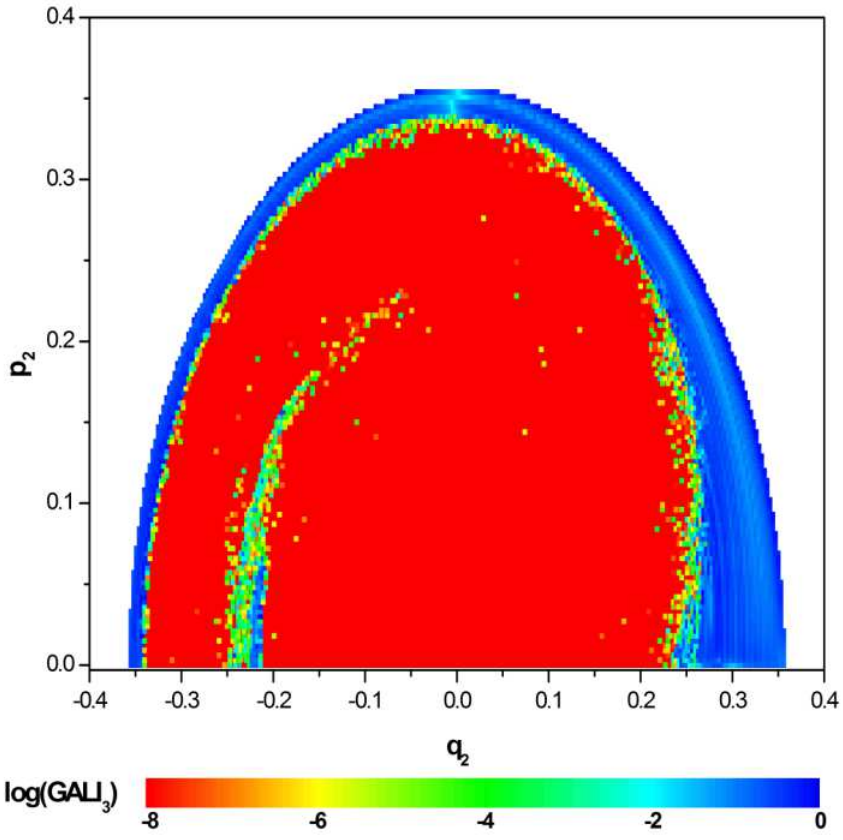

Global dynamics

$GALI_k$ with k>N

The index tends to zero both for regular and chaotic orbits but with completely different time rates:

Chaotic motion: exponential decay

Regular motion: power law

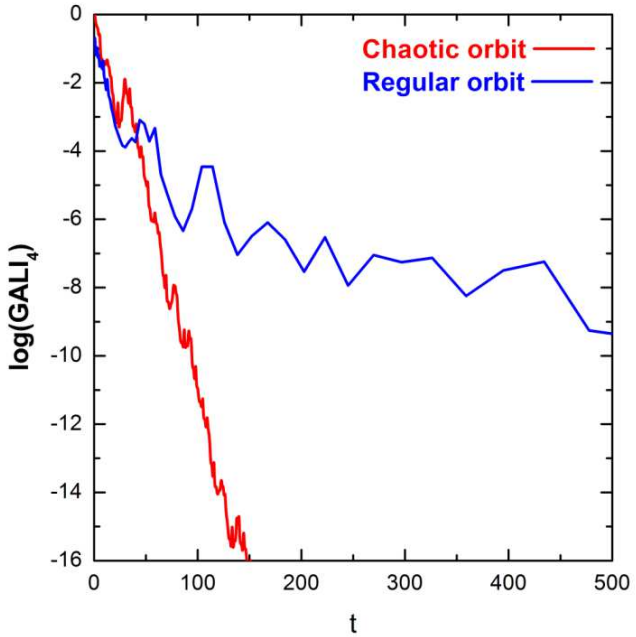

2D Hamiltonian (Hénon-Heiles)
Time needed for $GALI_4<10^{-12}$

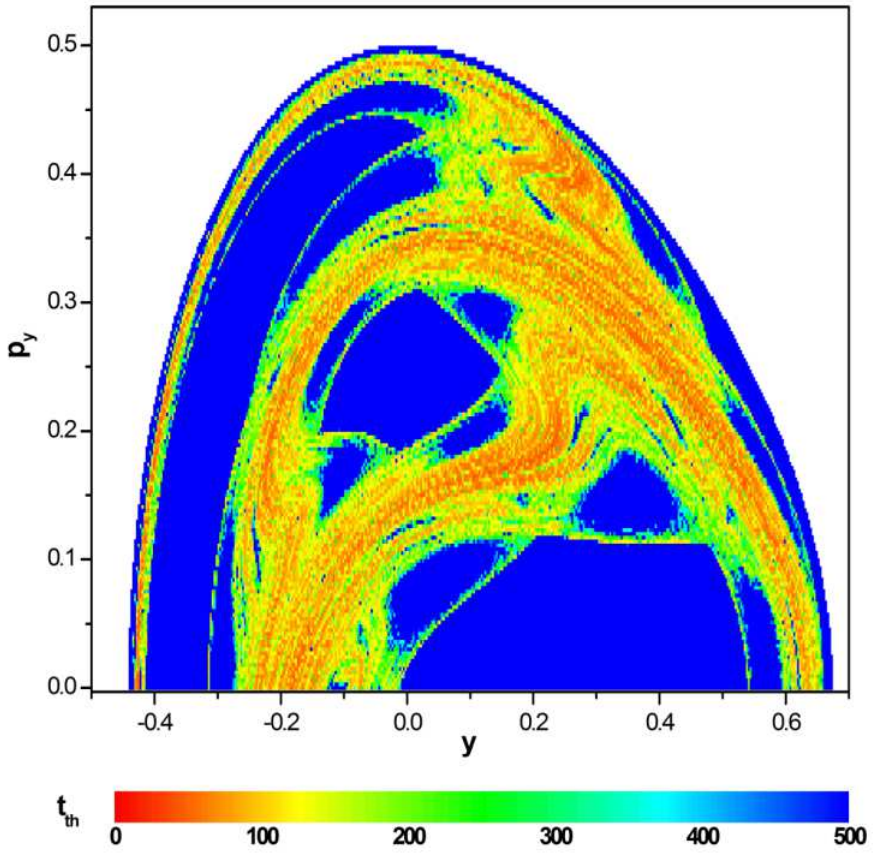

Behavior of $GALI_k$

Chaotic motion:

$GALI_k \rightarrow 0$ exponential decay

$$GALI_k(t) \propto e^{-\left[(\sigma_1-\sigma_2)+(\sigma_1-\sigma_3)+\ldots+(\sigma_1-\sigma_k)\right]t}$$

Regular motion:

$GALI_k \rightarrow$ constant $\neq 0$ or $GALI_k \rightarrow 0$ power law decay

$$GALI_k(t) \propto \begin{cases} \text{constant} & \text{if} \quad 2 \le k \le s \\ \dfrac{1}{t^{k-s}} & \text{if} \quad s < k \le 2N-s \\ \dfrac{1}{t^{2(k-N)}} & \text{if} \quad 2N-s < k \le 2N \end{cases}$$

Regular motion on low-dimensional tori

A regular orbit lying on a 2-dimensional torus for the N=8 FPU system.

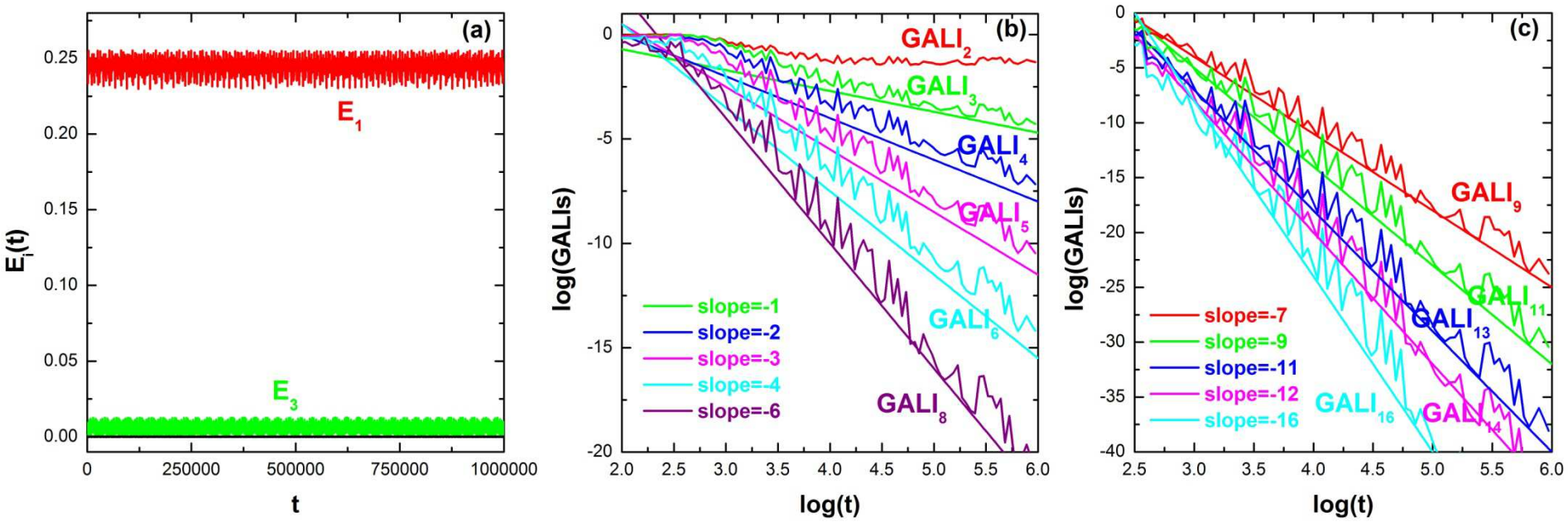

Regular motion on low-dimensional tori

A regular orbit lying on a 4-dimensional torus for the N=8 FPU system.

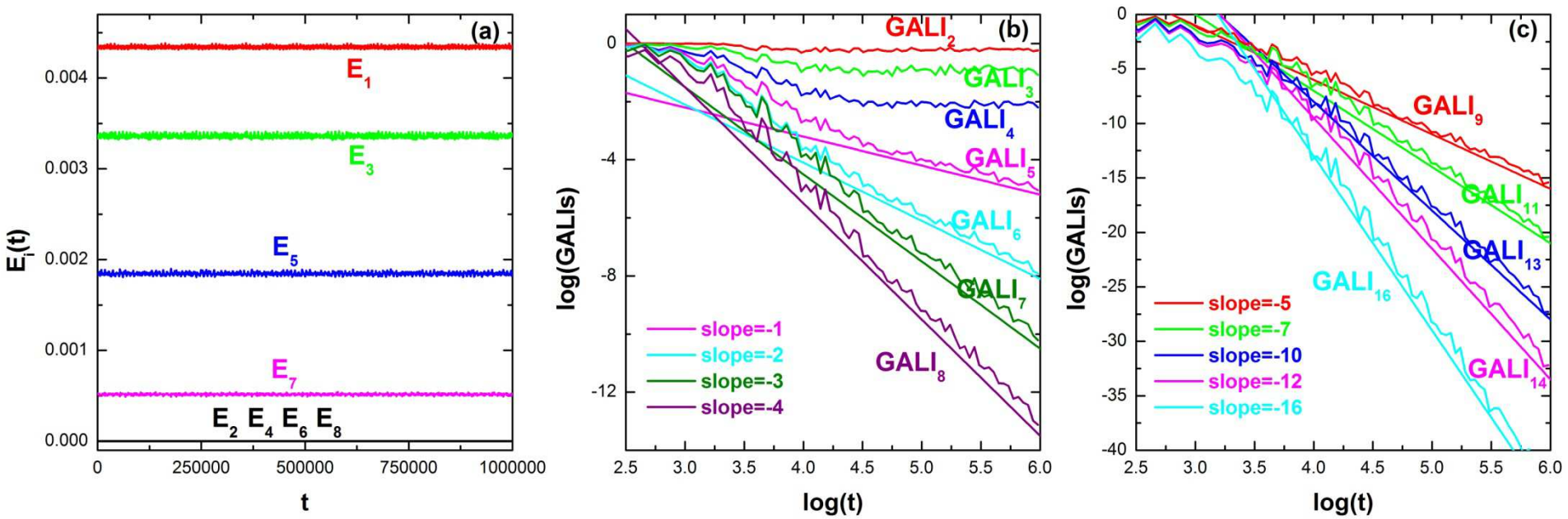

Locating low-dimensional tori

Orbits with $q_1=q_2=0.1$, $p_1=p_2=p_3=0$, H=0.010075 for the N=4 FPU system (Gerlach, Eggl, Ch.S., 2012, Int. J. Bif. Chaos).

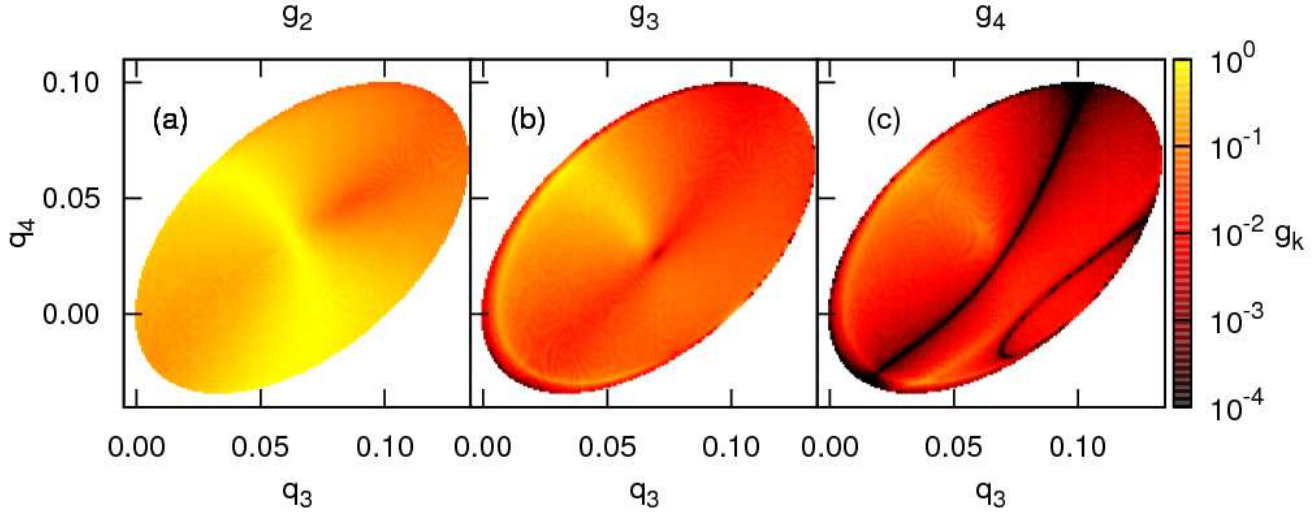

$$g_k = \frac{\mathrm{GALI}_k}{\max(\mathrm{GALI}_k)}$$

Locating low-dimensional tori

Orbits with $q_1=q_2=0.1$, $p_1=p_2=p_3=0$, H=0.010075 for the N=4 FPU system (Gerlach, Eggl, Ch.S., 2012, Int. J. Bif. Chaos).

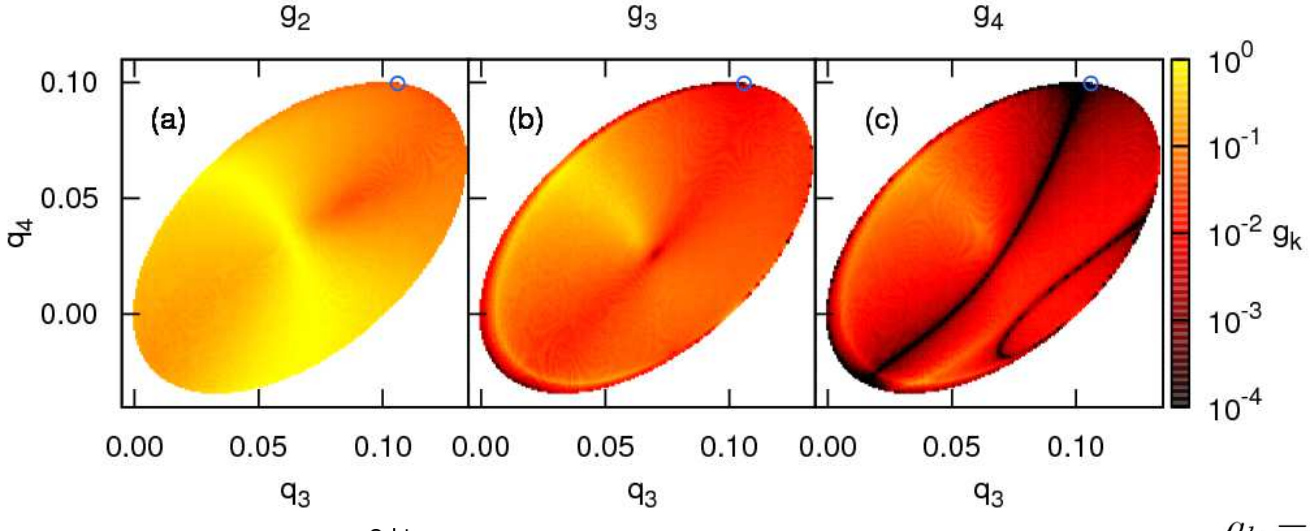

$$g_k = \frac{\mathrm{GALI}_k}{\max(\mathrm{GALI}_k)}$$

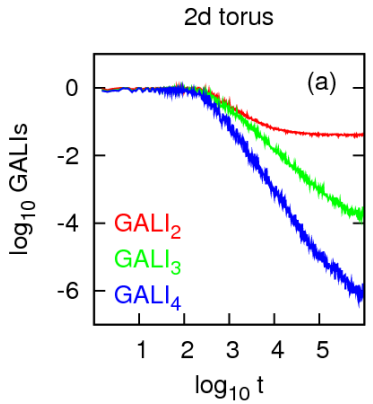

Locating low-dimensional tori

Orbits with $q_1=q_2=0.1$, $p_1=p_2=p_3=0$, H=0.010075 for the N=4 FPU system (Gerlach, Eggl, Ch.S., 2012, Int. J. Bif. Chaos).

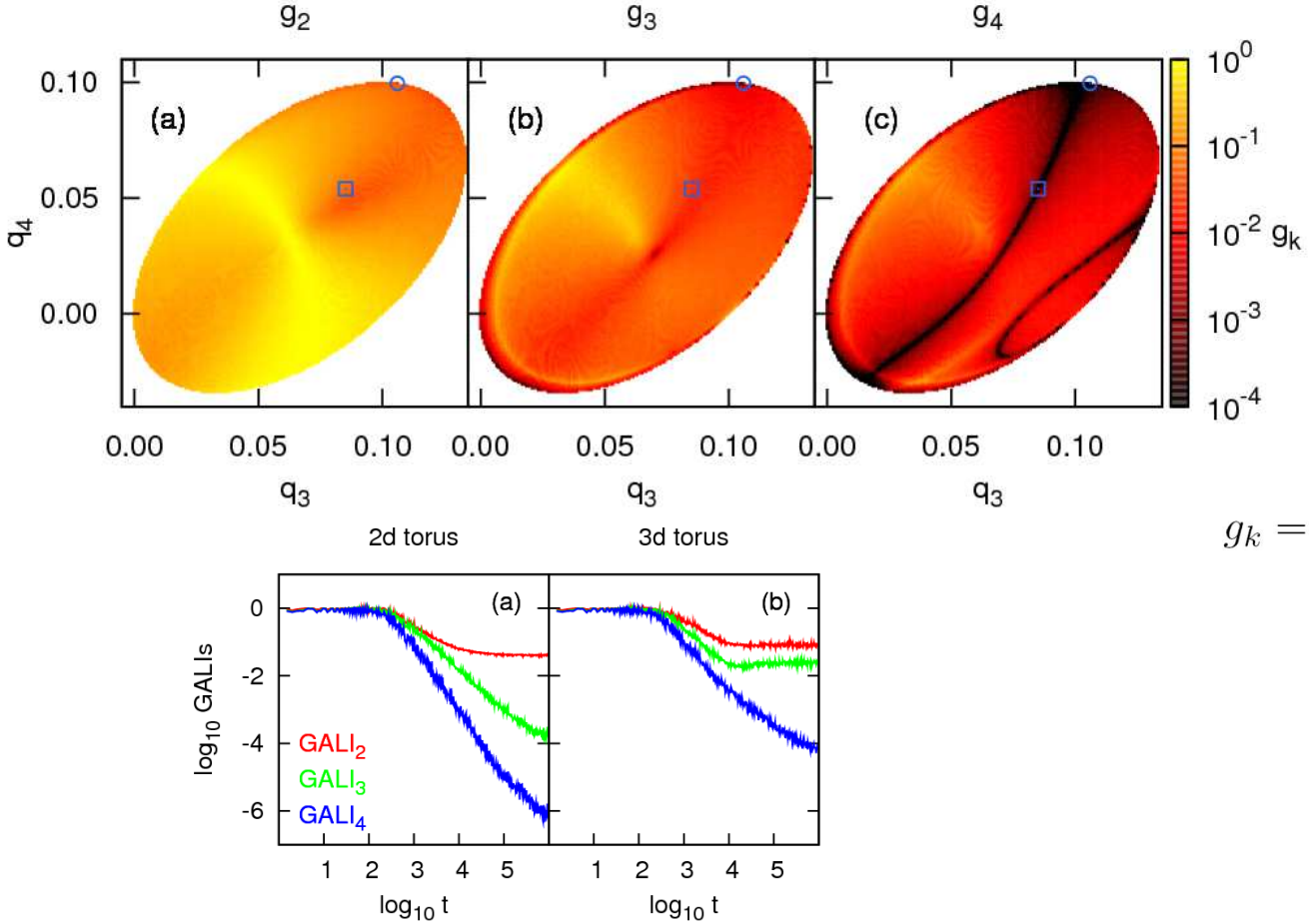

$$g_k = \frac{\mathrm{GALI}_k}{\max(\mathrm{GALI}_k)}$$

Locating low-dimensional tori

Orbits with $q_1=q_2=0.1$, $p_1=p_2=p_3=0$, H=0.010075 for the N=4 FPU system (Gerlach, Eggl, Ch.S., 2012, Int. J. Bif. Chaos).

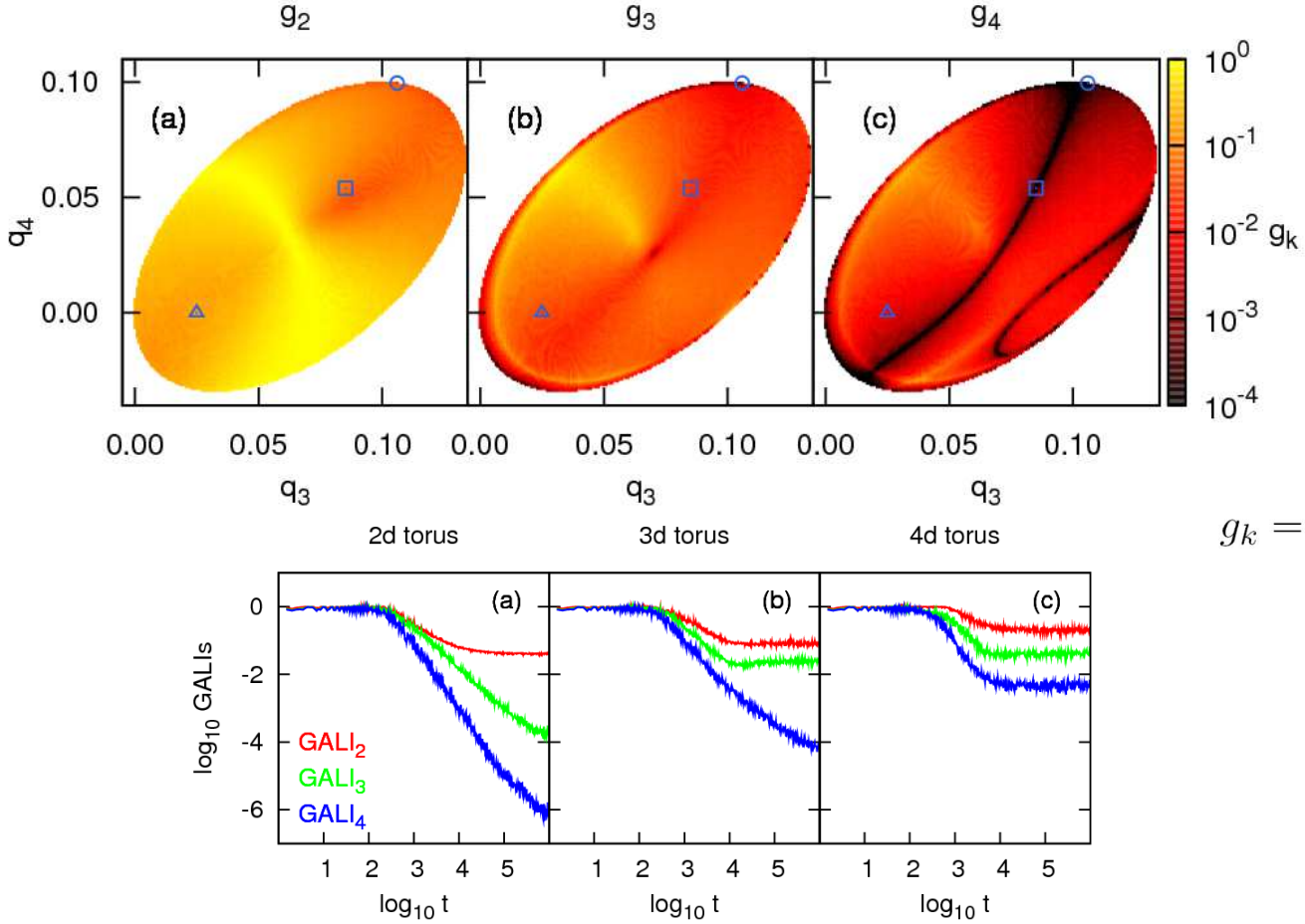

$$g_k = \frac{\mathrm{GALI}_k}{\max(\mathrm{GALI}_k)}$$

Summary

- **$GALI_k$ indices :**
  - ✓ **can distinguish rapidly and with certainty between regular and chaotic motion**
  - ✓ **can be used to characterize individual orbits as well as "chart" chaotic and regular domains in phase space.**
  - ✓ **are perfectly suited for studying the global dynamics of multidimentonal systems**
  - ✓ **can identify regular motion on low–dimensional tori**

- **SALI/GALI methods have been successfully applied to a variety of conservative dynamical systems of**
  - ✓ **Celestial Mechanics (e.g. Széll et al., 2004, MNRAS - Soulis et al., 2008, Cel. Mech. Dyn. Astr. - Libert et al., 2011, MNRAS)**
  - ✓ **Galactic Dynamics (e.g. Capuzzo-Dolcetta et al., 2007, Astroph. J. - Carpintero, 2008, MNRAS - Manos & Athanassoula, 2011, MNRAS)**
  - ✓ **Nuclear Physics (e.g. Macek et al., 2007, Phys. Rev. C - Stránský et al., 2007, Phys. Atom. Nucl. - Stránský et al., 2009, Phys. Rev. E)**
  - ✓ **Statistical Physics (e.g. Manos & Ruffo, 2010, Trans. Theory Stat. Phys.)**

Main references

- **Bountis T.C. & Ch.S. (2012) 'Complex Hamiltonian Dynamics', Chapter 5, Springer Series in Synergetics**

- **SALI**
  - ✓ **Ch.S. (2001) J. Phys. A, 34, 10029**
  - ✓ **Ch.S., Antonopoulos Ch., Bountis T. C. & Vrahatis M. N. (2003) Prog. Theor. Phys. Supp., 150, 439**
  - ✓ **Ch.S., Antonopoulos Ch., Bountis T. C. & Vrahatis M. N. (2004) J. Phys. A, 37, 6269**
  - ✓ **Bountis T. & Ch.S. (2006) Nucl. Inst Meth. Phys Res. A, 561, 173**
  - ✓ **Boreaux J., Carletti T., Ch.S. &Vittot M. (2012) Com. Nonlin. Sci. Num. Sim., 17, 1725**
  - ✓ **Boreaux J., Carletti T., Ch.S., Papaphilippou Y. & Vittot M. (2012) Int. J. Bif. Chaos, 22, 1250219**

- **GALI**
  - ✓ **Ch.S., Bountis T. C. & Antonopoulos Ch. (2007) Physica D, 231, 30-54**
  - ✓ **Ch.S., Bountis T. C. & Antonopoulos Ch. (2008) Eur. Phys. J. Sp. Top., 165, 5-14**
  - ✓ **Gerlach E., Eggl S. & Ch.S. (2012) Int. J. Bif. Chaos, 22, 1250216**
  - ✓ **Manos T., Ch.S. & Antonopoulos Ch. (2012) Int. J. Bif. Chaos, 22, 1250218 [Behavior of GALI for periodic orbits]**
  - ✓ **Manos T., Bountis T. & Ch.S. (2013) J. Phys. A, 46, 254017 [Behavior of GALI for time dependent Hamiltonians]-> Talk of T. Manos on Thursday 20 June**